remote sensing

MDPI

Article

The Impact of Vegetation on the Visibility of Archaeological Features in Airborne Laser Scanning Datasets from Different Acquisition Dates

Michael Doneus [1,2,*], Łukasz Banaszek [3] and Geert J. Verhoeven [4]

[1] Department of Prehistoric and Historical Archaeology, University of Vienna, Franz-Klein-Gasse 1, 1190 Vienna, Austria
[2] Human Evolution & Archaeological Sciences (HEAS), University of Vienna, Universitätsring 1, 1010 Vienna, Austria
[3] Historic Environment Scotland, John Sinclair House, 16 Bernard Terrace, Edinburgh EH8 9NX, UK; lukasz.banaszek@hes.scot
[4] Ludwig Boltzmann Institute for Archaeological Prospection and Virtual Archaeology, Hohe Warte 38, 1190 Vienna, Austria; geert.verhoeven@archpro.lbg.ac.at
* Correspondence: michael.doneus@univie.ac.at

Abstract: Digital elevation models derived from airborne laser scanning have found worldwide application in archaeology and other disciplines. A key feature that makes these models so valuable lies in their capacity to represent micro-relief features indicating traces of past human activity. While detection of these often faint traces in vegetated areas benefits from maximum leaf-off conditions during data acquisition, countrywide collection of data must make compromises and often cannot take place in the most appropriate seasons. In this paper, we identify the impact of leaf-on conditions on the distribution of ground returns and present what types of archaeological objects might remain unnoticeable if the flight date is outside the desirable time window. Comparing five ALS data acquisition campaigns from both leaf-off (April and November) and leaf-on conditions (May and June), we demonstrate how foliage affects the morphology of relief features as recorded in ALS derivatives, and we identify other effects on archaeological interpretation caused by changing vegetation conditions. The results encourage evaluation of countrywide general-purpose data for their applicability in archaeology.

Keywords: airborne laser scanning; vegetation impact; interpretative mapping; comparison of datasets; visibility of archaeological features

Citation: Doneus, M.; Banaszek, Ł.; Verhoeven, G.J. The Impact of Vegetation on the Visibility of Archaeological Features in Airborne Laser Scanning Datasets from Different Acquisition Dates. *Remote Sens.* **2022**, *14*, 858. https://doi.org/10.3390/rs14040858

Academic Editor: Devrim Akca

Received: 13 January 2022
Accepted: 9 February 2022
Published: 11 February 2022

1. Introduction

Airborne Laser Scanning (ALS, also known as airborne lidar) has found wide application in archaeology, proving to be an efficient method for documenting relief features over large, even vegetated areas [1–7]. ALS data are often collected countrywide by order of governmental organisations and usually made available as georeferenced and filtered point clouds or various ALS derivatives. Very often, these datasets are affordable or even provided for free [8–10]. One must, however, note that their production is a complex process involving a range of assumptions, decisions, and compromises throughout the workflow of project preparation, data acquisition, processing, and visualization [7,11,12].

Several factors affect the quality of ALS products, including the flying platform and scanning device, survey parameters (i.e., opening angle, pulse rate, field of view, flying height above ground level, overlap between neighbouring scan stripes, flying velocity), date and time of data acquisition, point cloud extraction algorithms (whenever a full-waveform scanner is in operation), and geo-referencing techniques, as well as software and parameters used for data filtering and classification [13–16]. There are also other, uncontrolled factors, such as wind speed during flight, land-use and land-management practices, or

general topography. In addition, the quality of ALS-derived digital terrain, surface, and feature models (DTM, DSM and DFM, respectively) not only builds on the characteristics of the point cloud but also results from algorithms and algorithm-specific parameters (e.g., software and parameter settings used for classification [16,17]) and interpolation methods [18], including the cell size of the output raster. Finally, the potential of ALS in revealing archaeological features and understanding the landscape is also determined by subjective processes involved in data interpretation: research goals; visualisation techniques [19–22]; experience; a-priori information; power-knowledge relation or intuition [23–26].

While the effect of some of these parameters has been the subject of investigations [6,7,11,16,18,27], no research has been published on the impact that the data acquisition date has on the detectability of archaeological features. Nonetheless, data from leaf-on and leaf-off conditions were tested and used to map and model tree species ([28] with further references on p. 1500). Variability in vegetation cover and its impact on the distribution of ground points has been investigated for the Forest of Dean for discrete return lidar systems, showing that dense understorey (bramble and/or bracken fronds) and dense conifer plantations notably obstruct the visibility of round features, such as charcoal burning platforms [5]. In addition, the impact of tree species on the distribution of ALS point data has been identified for the mixed woodland of the North European Plain [29,30]. In the case of rain forests of South- and Mesoamerica and South-East Asia, due to the evergreen nature of the forest, acquisition dates are rarely discussed [31–36]. Nonetheless, Evans [37] mentions that data acquisition in Cambodia should take place at the end of the dry season due to the "peak 'leaf-off' conditions in deciduous trees" at this time. Cap et al. [38] argue in a similar way for scans in Belize. Fernandez-Diaz et al. [6] report on lidar canopy penetration in Mesoamerica, giving a detailed assessment on sensor configuration and flight parameters, but do not discuss the acquisition date.

While it seems to be general knowledge that in temperate climates data acquisition should take place in leaf-off conditions (mostly winter to early spring) with no snow on the ground to produce optimal results, operating only in leaf-off conditions leads in some areas to very short operational windows. For instance, in Scandinavia or high alpine regions, long snowy winters require scheduling of acquisition flights in late spring when deciduous trees produce leaves [2]. Therefore, it is unsurprising that extensive data acquisition projects are likely to cover large areas outside the ideal time window. While this may still yield satisfactory outputs for archaeological purposes, the understanding of the reduction in the archaeological information due to tree foliation is key to assess the archaeological usability of such datasets.

This paper identifies the impact of leaf-on conditions on the distribution of survey points and discusses the types of archaeological features that may go unnoticed if the flight date is outside an optimal time window. In addition, by investigating a few ALS datasets, the impact of foliage on the morphology of relief features as recorded in ALS derivatives is discussed, also identifying other changes to archaeological interpretation caused by varying vegetation conditions. After presenting the case study area (Section 2), we discuss the parameters of the ALS data acquisition campaigns (Section 3) and the comparison methodology (Section 4). The results (Section 5) demonstrate the significant impact of specific vegetation conditions on the recorded morphology and detectability of archaeological features. These are later discussed (Section 6) and conclusively summarised (Section 7).

2. Case Study Area

Located some 30 km southeast of Vienna in the shadow of the Leitha Mountains (Leithagebirge) on the border between the Austrian federal states of Lower Austria and Burgenland (Figure 1), St. Anna in der Wüste has been a focus for a methodological research on archaeological ALS for more than a decade [39–43]. Since 2007, the area has been repeatedly documented throughout different seasons, including less favourable periods of the year, as part of the research programme of the Ludwig Boltzmann Institute

for Archaeological Prospection and Virtual Archaeology (LBI ArchPro) [44]. This makes it an ideal case study for investigating the impact of canopy density on the detectability of archaeological features in woodland.

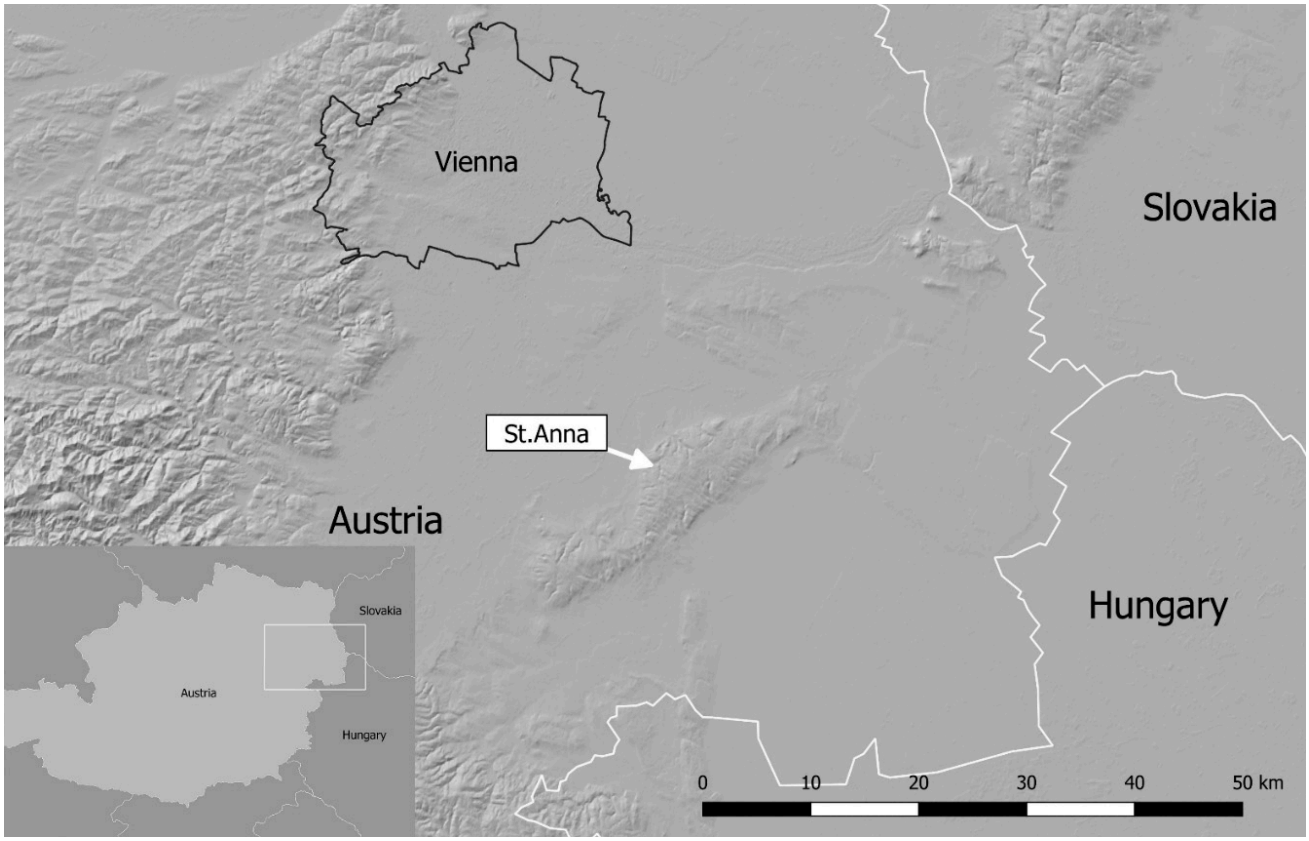

Figure 1. Location of the study area.

The area is rich with different types of archaeological sites in various states of preservation, with the ruins of a medieval friary complex forming the most prominent structure surviving in the landscape. While the church and some parts of the friary complex (Figure 2a) are well preserved, other features are either largely ruined (e.g., Castle of Scharfeneck—Figure 2b, former farmhouse—Figure 2c, hermits' cells—Figure 2d) or buried, the latter leaving only faint relief traces. The area comprises also banks and ditches of a prehistoric hillfort (Figure 2e), round barrows (Figure 2f), old trackways (Figure 2g), former quarries (Figure 2h) and fishponds (Figure 2i), as well as the evidence of a field system (Figure 2j).

Most of the archaeological features are enclosed within a managed deciduous forest dominated by oak, beech, and hornbeam. Robinia and hazel are also present in the area with a varying degree of understorey, which includes nettle, wild garlic, and ivy. Unsurprisingly, the age of the trees, species structure, and vegetation density varies. This is a result of historic and contemporary forest management practices and other human actions, the presence of anthropogenic features, the concomitance of particular plants, soil distribution, and other natural factors.

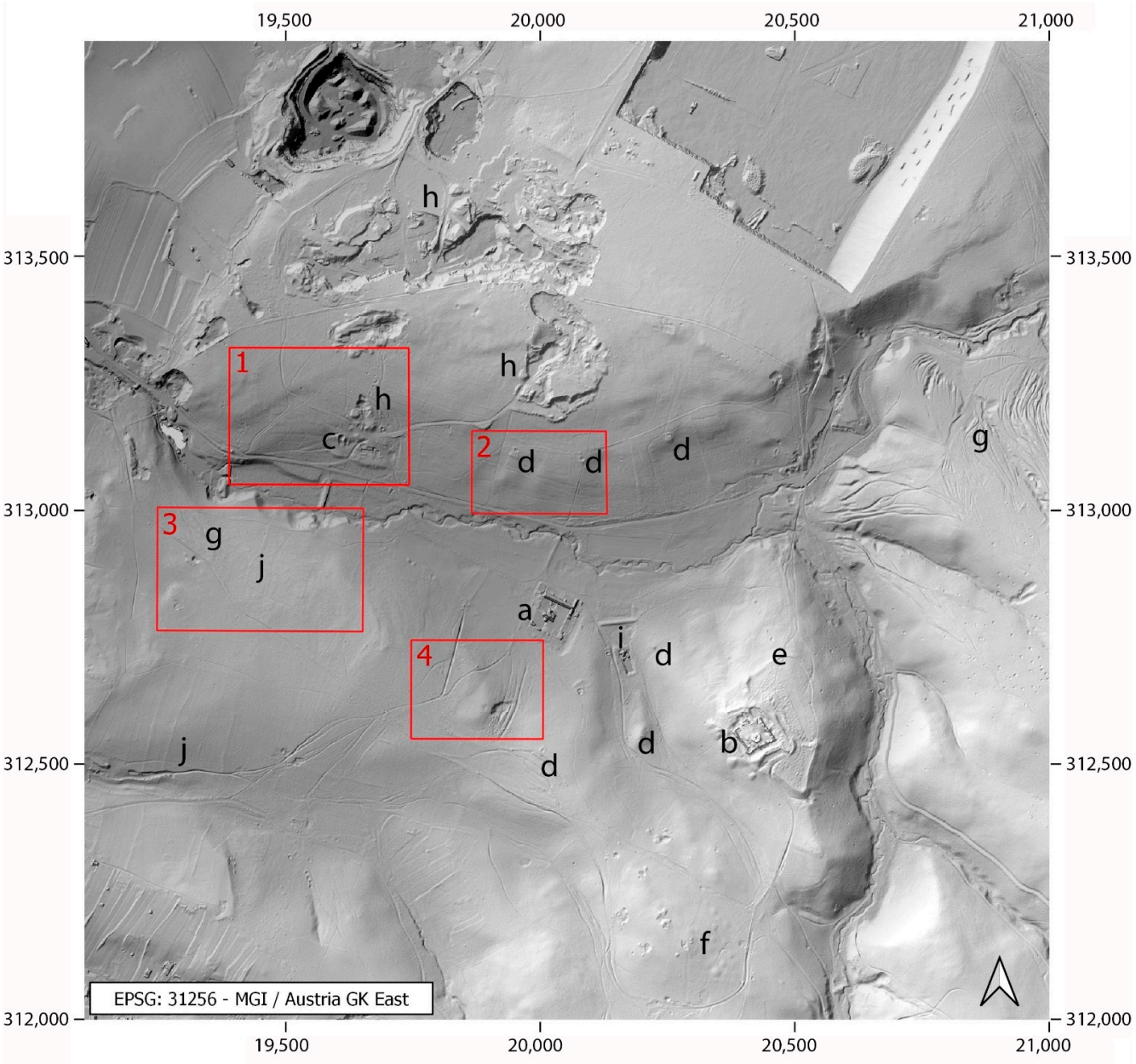

Figure 2. Various types of archaeological features located in the St. Anna area. Hillshade visualisation of data acquired in Spring 2007. The red boxes indicate the location of sample zones fully interpreted archaeologically (1–4). (**a**) friary complex, (**b**) Castle of Scharfeneck, (**c**) former farmhouse, (**d**) hermit's cells, (**e**) prehistoric hillfort, (**f**) barrows, (**g**) trackways, (**h**) quarries, (**i**) fishponds, (**j**) field system.

3. Data and Metadata

The data used in this study result from five archaeological data acquisition campaigns undertaken in 2007, 2010, 2011, and 2012 (Figure 3). In terms of seasons, flights were conducted in March/April, May, June and November. The parameters of each flight are listed in Table 1.

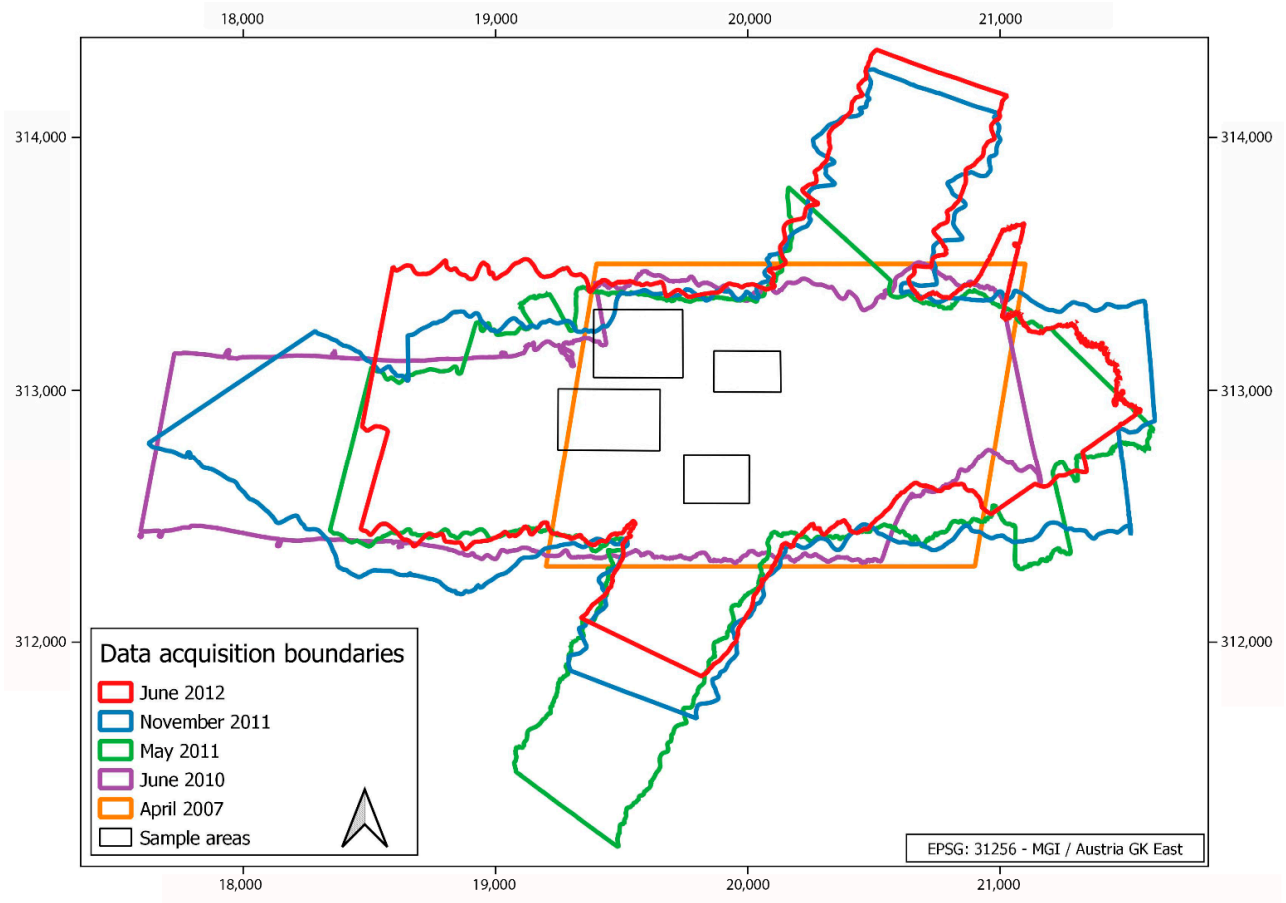

Figure 3. Coverage of individual ALS surveys.

Table 1. Parameters of all ALS flights used in this paper.

ALS-Project	Leithagebirge	LBI ArchPro—St. Anna	LBI ArchPro—St. Anna	LBI ArchPro—St. Anna	LBI ArchPro—St. Anna
Purpose of scan	Archaeology	Archaeology (spectroscopy)	Archaeology	Archaeology	Archaeology
Time of data acquisition	26 March–12 April 2007	9 June 2010	26 May 2011	11 November 2011	18 June 2012
Mean point density of return (all echoes) per m^2	17	5	33.5	21.5	25.7
Mean point density of last echoes per m^2	9.7	3	22.8	13.1	15.1
Ground points (after filtering) per m^2	5.4	0.5	1.5	4.4	2.2
Strip overlap	70%	70%	70%	70%	70%
Scanner type	Riegl LMS-Q560 Full-Waveform	Riegl LMS-Q680i Full-Waveform	Riegl LMS-Q680i Full-Waveform	Riegl LMS-Q680i Full-Waveform	Riegl LMS-Q680i Full-Waveform
Scan angle (whole FOV)	45°	60°	60°	60°	60°
Flying height above ground	600 m	450 m	450 m	450 m	450 m
Speed of aircraft (TAS)	70 kts (36 m/s)	98 kts (50 m/s)	98 kts (50 m/s)	98 kts (50 m/s)	98 kts (50 m/s)
Laser pulse rate	100,000 Hz	400,000 Hz	400,000 Hz	400,000 Hz	400,000 Hz
Scan rate	66,000 Hz	140,000 Hz	400,000 Hz	400,000 Hz	400,000 Hz
Strip adjustment	Yes	Yes	Yes	Yes	Yes
Filtering	Robust interpolation (OPALS)	Robust interpolation (OPALS)	Robust interpolation (OPALS)	Robust interpolation (OPALS)	Robust interpolation (OPALS)
DTM cell size	0.5 m	1 m	0.5 m	0.5 m	0.5 m

Unlike the experiments conducted by Fernandez-Diaz et al. [6], we do not attempt to find parameters for optimal canopy penetration. We rather use similar acquisition parameters to compare the quality of archaeological information resulting from the acquired datasets. While all survey campaigns were undertaken with full-waveform scanners, the Spring 2007 flight, one of the first full-waveform campaigns for archaeological purposes, and the June 2010 survey, which foregrounded the acquisition of imaging spectroscopy data, demonstrate slightly different flight parameters. In each case a strip overlap of 70% was planned to achieve higher point densities and to allow fine strip adjustment [11].

Field visits to the study area were undertaken to assess and record the conditions of ground cover. Unfortunately, photographs at the actual date of data acquisition were taken only during the 2007 survey (Figure 4, upper row). After an unusually mild winter, the vegetation period had already started at the beginning of April. Leaves began to appear, and wild garlic covered large parts of the study area. In all other cases, ground photographs were not taken together with the ALS survey but at a similar date in the following years. Although this may have caused slight differences while investigating the autumnal environment (depending on the temperature, precipitation and wind conditions, the timing of defoliation may have been slightly earlier or later in 2011 than at the time of recording the ground conditions), it has not impacted the understanding of the scanning conditions in May and June when the foliage in this part of Austria is always vigorous.

Figure 4. On-site photographs. **Upper row**: Spring 2007; middle row: June 2013; **lower row**: November 2013 (photographs by M. Doneus).

4. Methodology

4.1. Point Cloud Processing and Density Maps

Prior to investigating the impact of leaf-on conditions on the recording of relief features, five ALS datasets were pre-processed. Echo detection, the generation of a 3D point

cloud from the scanner (direct geo-referencing of scan data by combining scanner range and deflection angle measurements and trajectory data derived from GNSS and inertial measurement devices), as well as strip adjustment were carried out using the OPALS software [45,46]. This initial processing step and all subsequent operations are depicted in the flowchart of Figure 5.

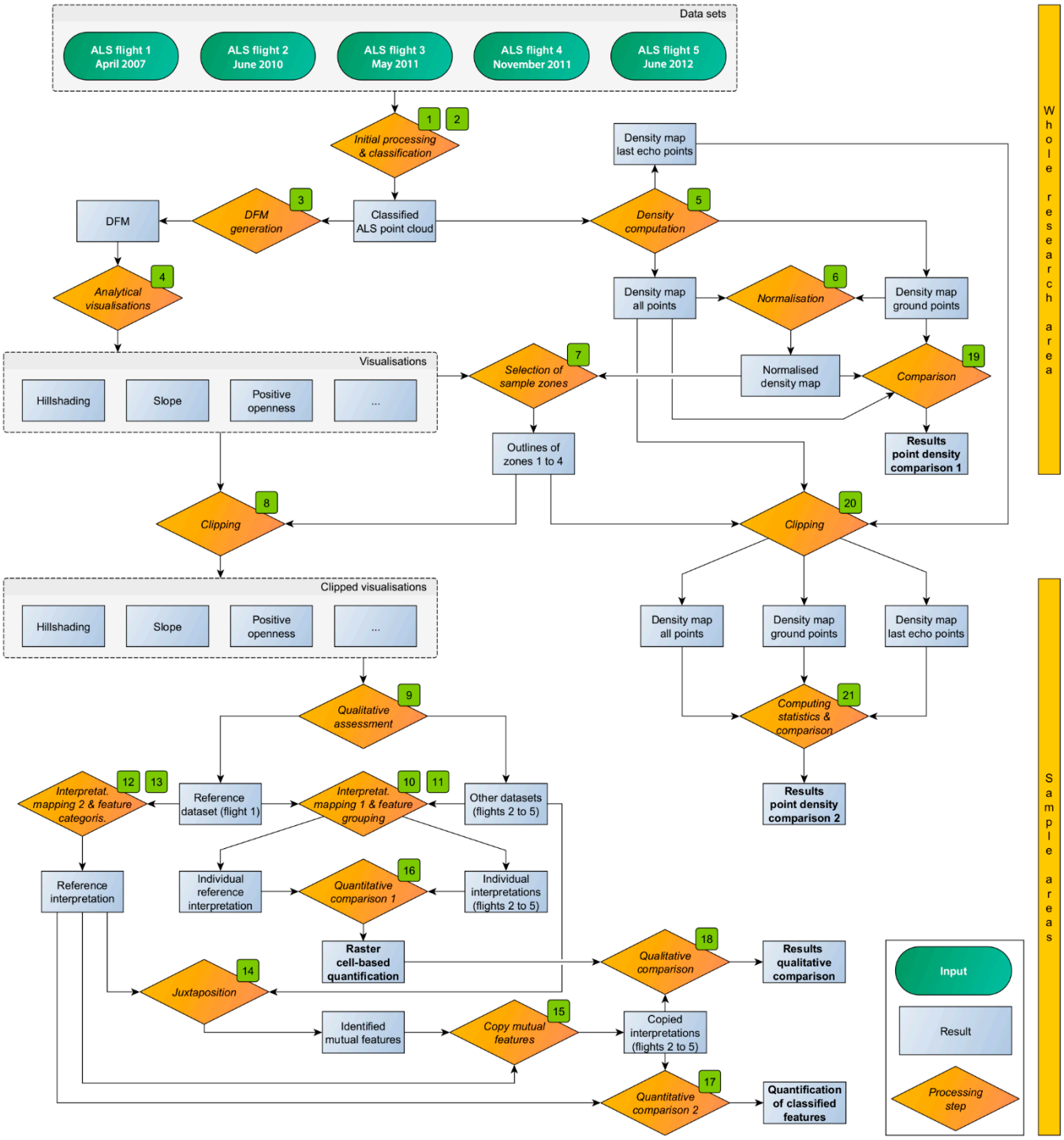

Figure 5. Diagram of the complete workflow described in the text.

Point clouds were classified using the software package SCOP++ and applying robust interpolation with an eccentric and unsymmetrical weight function (2 in Figure 5—for a more detailed explanation, see [17]). Ground points from the classified point cloud, as

well as points representing archaeologically relevant features, i.e., standing structures and earthworks (for the sake of convenience all these points are subsequently called "ground points"), were interpolated to produce a so called "feature DTM" or DFM [7,17,47] (3 in Figure 5). This was achieved using linear prediction [48], which is similar to Kriging and seems to maintain relief features even in reduced point clouds [6,27]. The same parameters were used to process each dataset. Subsequently, visualisation techniques (hillshading and slope, as well as positive and negative openness amongst others) were used to enhance the visibility of archaeological features (4 in Figure 5).

To understand the effect of vegetation on the visibility of archaeological features, three density maps were produced for each ALS dataset: (i) the density of all points in the cloud, (ii) the density of the classified ground points and (iii) of the last echoes (5 in Figure 5). The density maps clearly show that the distribution of lidar ground points was inconsistent even within the same ALS dataset. This is an effect of the varying forest structure. Additionally, the number of ground points was affected by the different data acquisition parameters (Table 1) and the layout of flight lines, with areas of overlapping strips demonstrating far higher point densities. To allow a coherent comparison of the different datasets, ground point density maps were normalised through division by the respective total ALS points density maps (6 in Figure 5).

These normalised outputs show the ground points density (points/m^2) with respect to the total number of digitised lidar pulses, and thus improve our understanding of the impact of off-ground obstacles on the capacity of ALS to record topographic features in different seasons. Figure 6, for example, indicates the forest horizontal and vertical structure. Bright areas illustrate a high percentage of off-ground points (i.e., a small percentage of actual ground points), and thus reveal, in some way, the presence of very dense and/or multistorey vegetation. Dark green, on the other hand, demarcates exposed areas.

4.2. Interpretation of Sample Areas

The analytical visualisations of the five DFMs and the respective normalised ground points density maps were used to evaluate the vertical and horizontal structure of each point cloud. Besides revealing the abundance of archaeological evidence and the complexity of the forest structure, this analysis also led to the definition of four sample areas (see red boxes in Figure 2 and 7 in Figure 5). The subsequent processing steps were confined to these four zones and all datasets were clipped (8 in Figure 5).

The DFM visualizations of the four sample areas were subjected to two archaeological interpretations. To compare these interpretations of all five datasets, a reference dataset had to be selected. The decision was made upon a qualitative assessment of the DFM visualisations (9 in Figure 5). Archaeological features seemed easiest to recognise in the Spring 2007 dataset, in which the distinct borders of even the slightest relief features can be observed. Although during this survey campaign Area 1 was uniformly covered with wild garlic (see Figure 4, upper right), a comparison with an older dataset from March 2006, which was not a subject of this study, demonstrated that this low vegetation had no effect on the recording of archaeological relief structures (see Abb. 9 in [40]).

While the visual assessment identified significant differences between the data acquired during leaf-on and leaf-off conditions, we also noticed some discrepancies between the results of the Spring 2007 campaign and the outcome of the November 2011 survey. In the latter case, features appeared a bit blurry and, in some areas, a misclassified clutter point resulted in DFM errors (e.g., in sample area 4). As a result, the Spring 2007 data became the reference dataset (i.e., dataset no. 1) against which other outputs of interpretative mapping were compared.

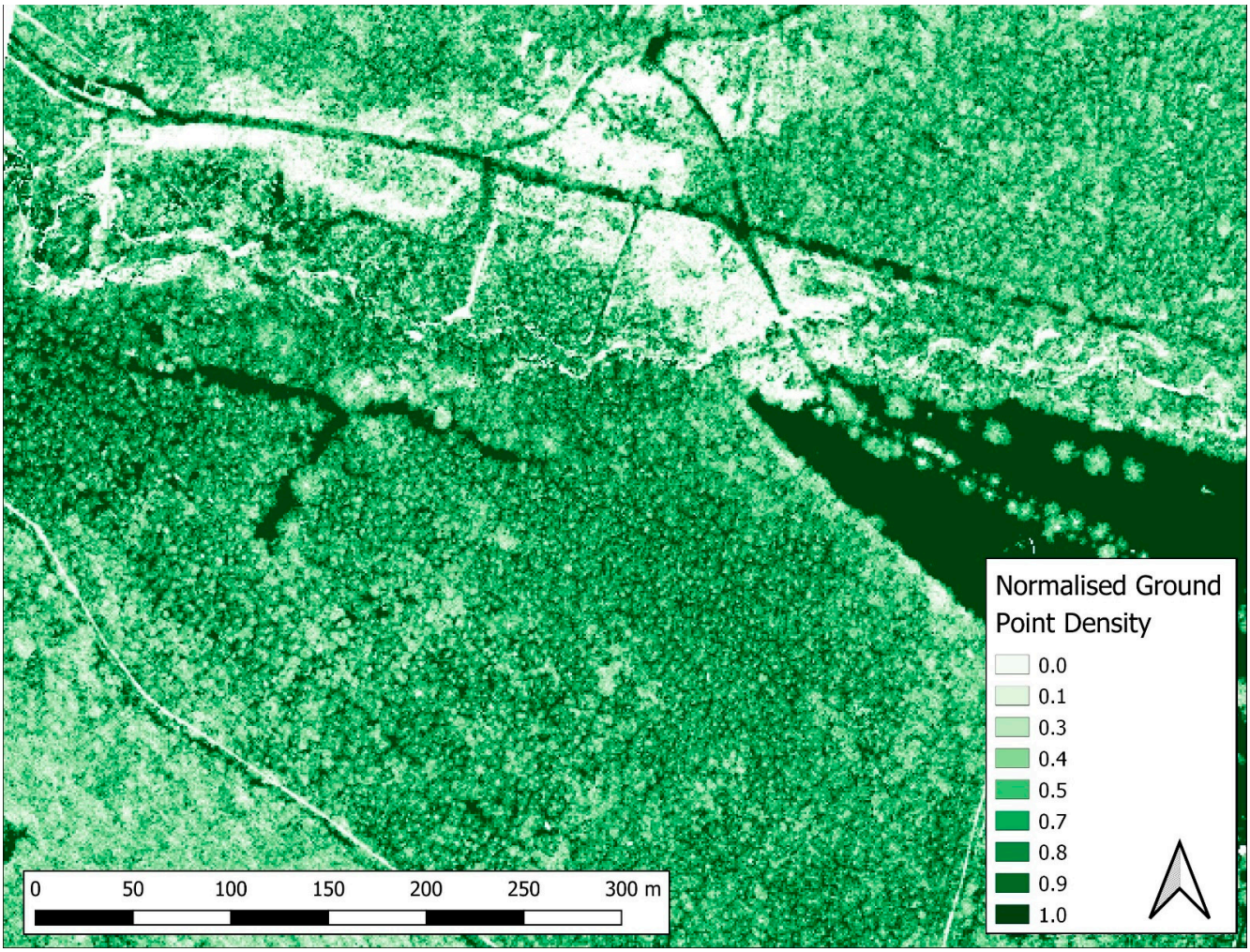

Figure 6. Normalised ground point density map from the data acquired in Spring 2007. Dark tones represent open areas (normalised ground point density = 1), while bright tones indicate dense vegetation.

The first of those interpretive mappings, in the following called "individual interpretation", was performed by one of the authors (LB). Each ALS dataset was addressed individually, which means that features were identified without referring to the interpretations of the other datasets. This workflow first resulted in the polygonization of the detected features (10 in Figure 5), which were afterwards grouped into several categories (see below) (11 in Figure 5). In this approach, the shape and size of the identified features was foregrounded, and less attention was paid to the archaeological classification. Structures recognized as resulting from modern forest management were ignored, and all sample areas were interpreted per each ALS dataset.

Due to the complexity of the identified archaeological features, summing up the absolute numbers of polygons (per zone per interpretation) to compare different datasets (see the Sections 5 and 6 below) was not an option. This would have led to quantification uncertainties, as it would have been almost impossible, for example, to consistently split up the complex networks of overlapping and intersecting hollow ways into individual features (Figure 7). Therefore, a second interpretation (12 in Figure 5) of the Spring 2007 reference dataset was undertaken by another author (MD). In this case, we were interested in tracking the individual features of complex archaeological structures. For instance, instead of interpreting a building as an area feature, individual walls were sketched. Five categories were distinguished: architecture (remains of buildings), area features (quarries, extraction pits, i.e., small quarries to extract stone material in close proximity to its use),

large pits, pits, and linear features (including roads, hollow ways, and field boundaries) (12 in Figure 5).

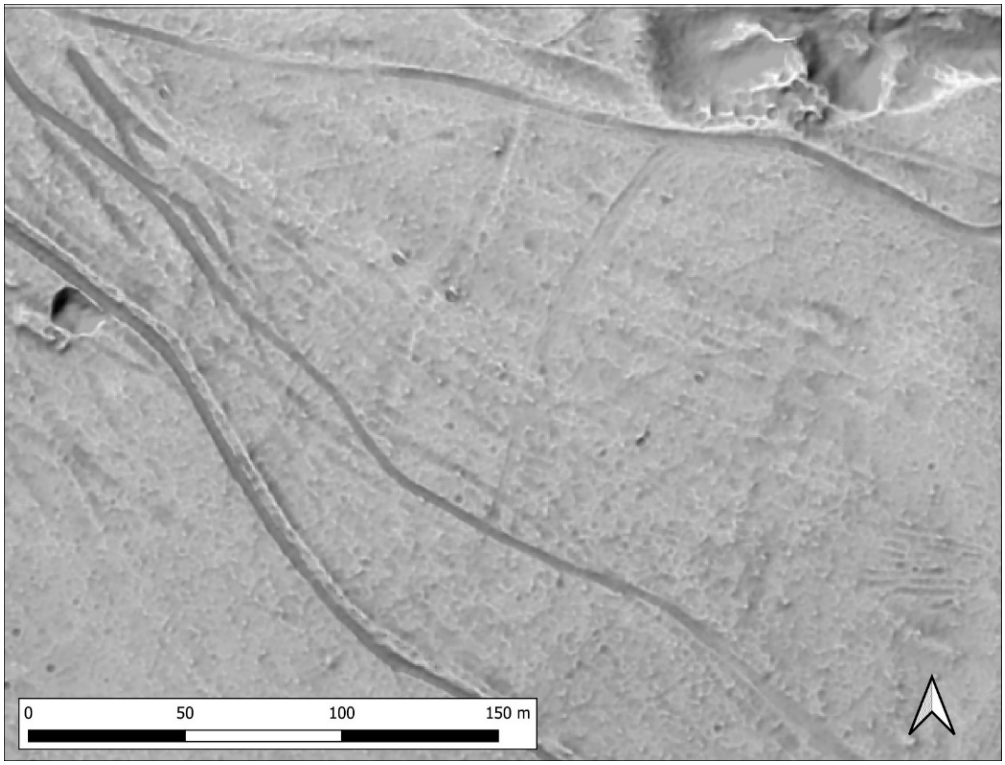

Figure 7. Positive openness visualisation of a part of the Area 3 showing part of a network of hollow ways cut into terrain by long-term repeated use in combination with rainwater runoff. Due to its complexity, it is almost impossible to consistently split this network into individual features when interpreting all datasets.

Thereafter, the polygons in all five categories were juxtaposed against the uninterpreted datasets of the subsequent ALS surveys (14 in Figure 5). In other words, we checked which archaeological features identified in the Spring 2007 reference data are visible in the datasets resulting from the other flights. Polygons representing such features were then copied from the reference interpretation to the respective dataset, thereby creating four so-called "copied interpretations" (15 in Figure 5). A positive openness visualisation (black to white colour gradient, linearly stretched between min. 1.41 and max. 1.58) was used to interpret all datasets. This ensured that the visibility of polygonised features was not distorted even in complex situations, such as in Figure 7. As a result, archaeological features could now be compared throughout the five datasets for each feature category by simply comparing the numbers of polygons.

4.3. Comparing the Outputs of Interpretation

The results of both interpretative mappings were subject to three comparisons. First, a quantitative approach addressed the outcomes of the "individual interpretations" on a raster cell basis (16 in Figure 5). A Python-based ArcGIS model was created to rasterize a user-specified pair of datasets, i.e., two polygon datasets resulting from the first interpretative mapping, and to compare both inputs cell by cell. Raster 1 represents reference archaeological information extracted from the Spring 2007 ALS data, with raster 2 holding the results of any of the four subsequent individual interpretations. The model developed converts the polygons to produce a binary raster for each set of interpretative outcomes with cell values of either '0' (feature absent) or '1' (feature present), assuming that all

vectorised features are archaeologically relevant. Next, these two rasters are compared. The output comparison raster (Figure 8) consequently builds on four cell values:

- '0' represents no archaeological information (no features identified in any of the compared rasters) in both datasets;
- '1' for features only detected in the reference raster (Spring 2007);
- '−1' for features only detected in raster no. 2;
- '2' for features detected in both rasters.

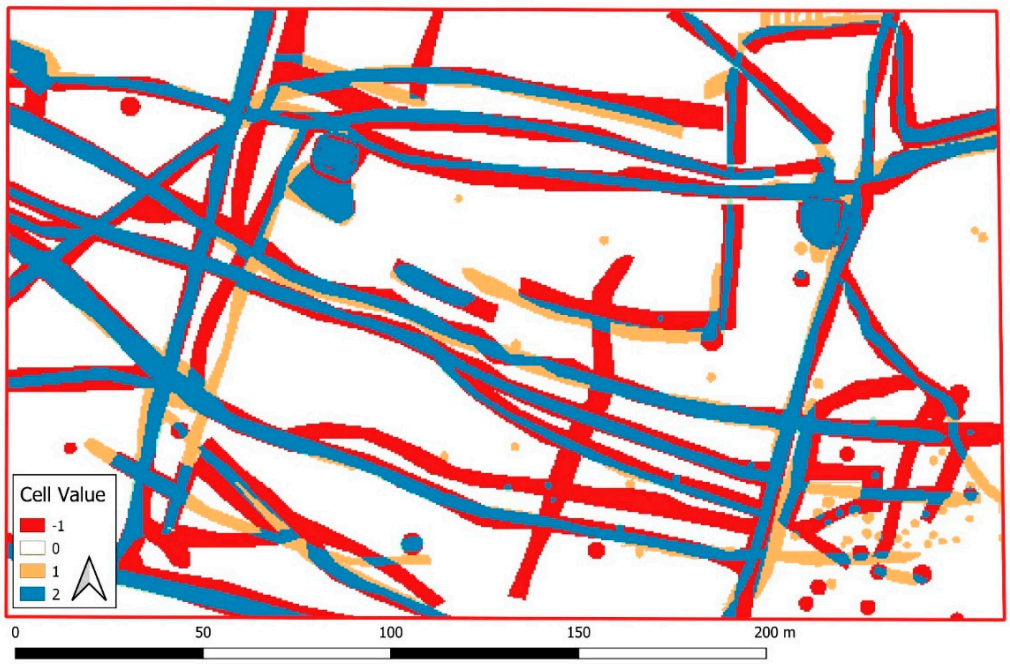

Figure 8. Comparison of Spring 2007 and 18 June 2012 datasets. Light orange features were detected solely in the older data, red exclusively in the later, and blue in both.

While this approach allowed for the quantification of all interpretations, the quality of such information is somehow restricted as the plethora of relief features can affect the computations. For example, the intertwinement of different object types (e.g., linear hollow ways and round pits) within an individual dataset may have some negative impact. Bomb craters and other small objects located within extensive features, such as sunken lanes or levelling platforms, were occluded, and hence "lost" in the quantification (Figure 9). To overcome this limitation, only two categories of archaeological features were selected from the interpretative mapping of sample areas for further analysis: linear features (aggregated hollow ways and field boundaries) and pits (e.g., extraction pits, kilns and bomb craters).

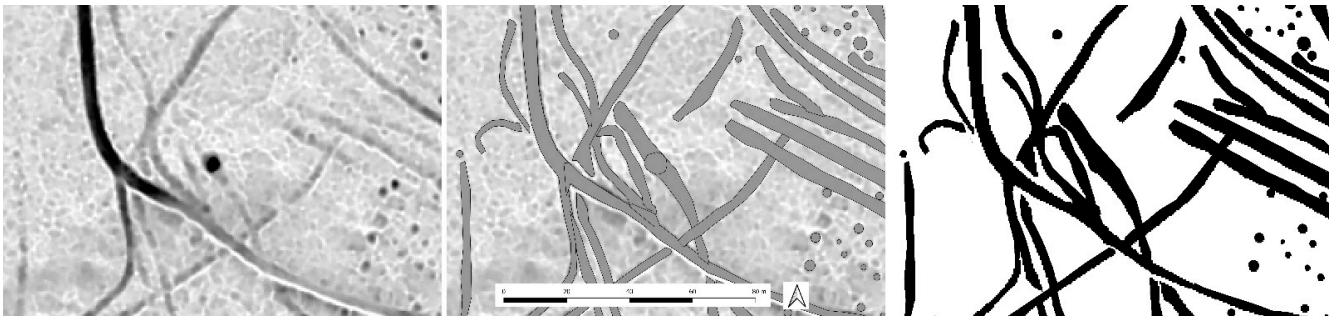

Figure 9. Occlusion of different types of features. A supposed bomb crater located within a hollow way (**left**) is somehow lost within the aggregated vector layer (**centre**) that was later rasterized (**right**).

The second, object-by-object, comparison built on the methodology of the "copied interpretation" (17 Figure 5). The number of features visible in each of the investigated datasets was compared for individual feature class and this approach used the five feature classifications.

While quantitative comparisons of interpretative mapping results indicate changes in morphology of the linear and pit-like features between different datasets, a detailed understanding of such changes may only be achieved by investigating the qualities of the identified features. Therefore, a final comparison of the datasets was qualitative and helped to improve our understanding of the loss of archaeological information between datasets collected at a different stage of vegetation development. This comparison builds on visual assessment of the investigated DFM visualisations and the results of interpretative mapping (18 in Figure 5).

5. Results

5.1. Point Density

The distribution of ALS survey points is an interplay between many factors, including flight parameters (such as flight height and velocity, pulse rate, opening angle, and strip overlap), the density and structure of vegetation/ground cover, and phenological state of vegetation. Because of these reasons, the investigated point clouds demonstrate considerable differences in point density, which are represented in Figure 10 (19 in Figure 5). To allow easier comparison, density maps are scaled from light green (0 pts/m^2) to dark green (>30 pts/ m^2) for both the total point density (left column) and ground point density (middle column). The lower total point density of flights undertaken in Spring 2007 and June 2010 are evident (cf. Table 1). In the former case, these result primarily from the lower 66 KHz scan rate and a higher altitude of survey flight, while the latter, also characterised by a low scan rate of 140 KHz, foregrounded the acquisition of data to produce a DSM for the orthorectification of simultaneously acquired imaging spectroscopy data. The total point density of the flights from May 2011, November 2011 and June 2012 are significantly higher. Indeed, for areas where survey strips overlap, the point density can reach over 100 points per m^2.

There are clear differences between total point density and ground point density for each survey. In the latter case, there are areas where 30 or more ground points per m^2 were recorded through the flights in May 2011, November 2011 and June 2012. However, for the May and June datasets, the high number of ground points comes from open areas, including the central meadow around the friary, while in the leaf-off conditions of November 2011 ground point density is generally high. The lowest ground point density was recorded for the June 2010 data, while the Spring 2007 flight recorded relatively uniform point density throughout the study area.

The right column of Figure 10 presents maps, scaled from light green (0) to dark green (1), of the normalised ground point density, i.e., the portion of ground points from the total points recorded per m^2. Outside the open areas where ground points were usually the only points recorded, the picture is quite different from the other columns. The leaf-off flights (Spring 2007 and November 2011) demonstrate relatively uniform high values, while the other flights are characterized by low ground point percentage in woodland areas and often null values were recorded for densely overgrown areas.

This is also reflected in Table 2, which presents the mean point density for all echoes, last echoes, and filtered ground points for four sample areas (20, 21 in Figure 5). While in all datasets the ratio of last echoes is about 50–60% of the total number of points recorded, there is a significant difference in the percentage of filtered ground points between the datasets. For the leaf-off period (March/April and November), the percentage of filtered ground points lies between 34% and 53%, while ground points were only a fraction—3% to 12%—of points recorded in May and June. The June 2010 flight demonstrates the lowest absolute values, which result also from the lower scan rate (compare Table 1).

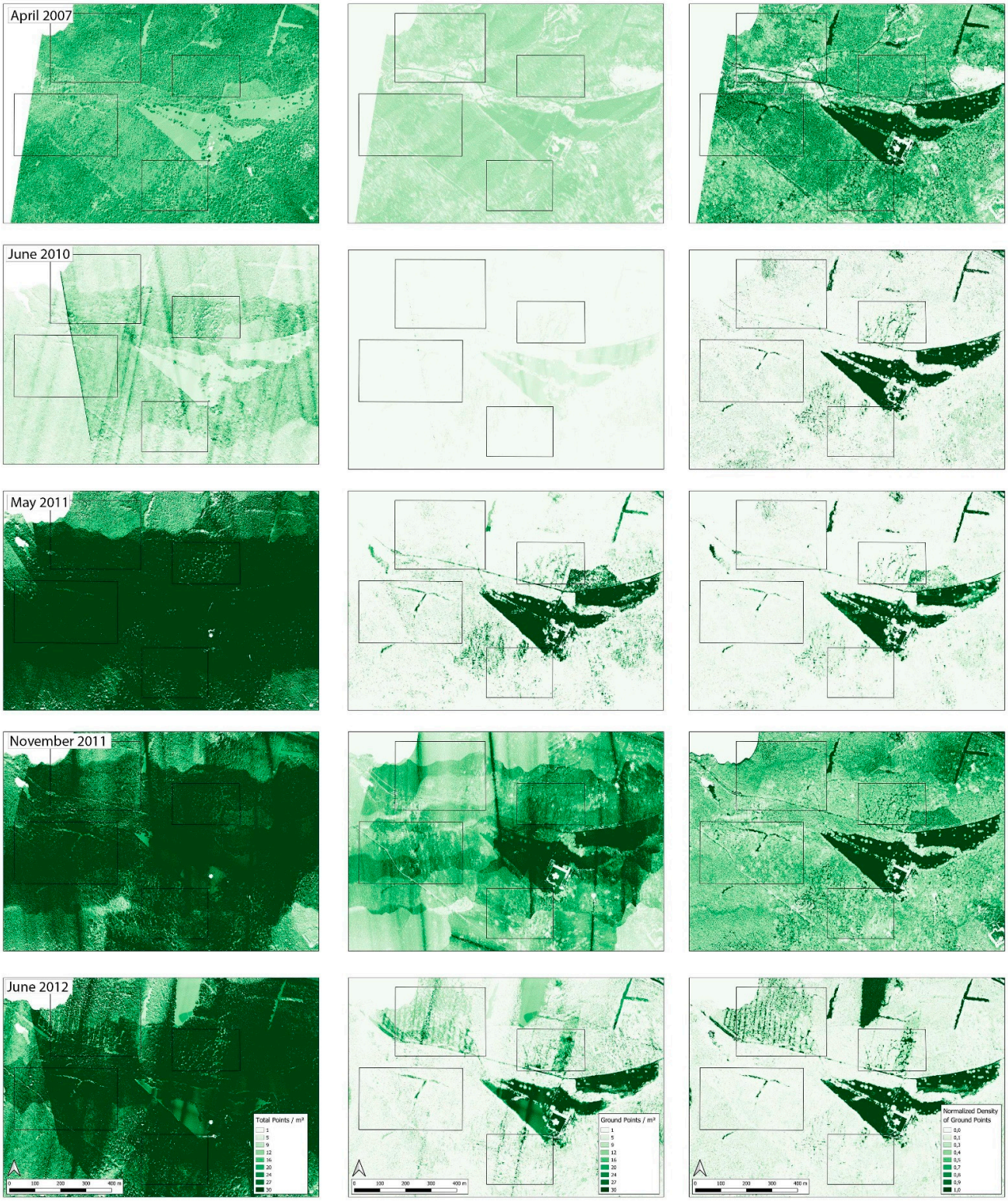

Figure 10. Point densities of all data acquisition flights. Left column: total point density; middle column: ground point density; right column: normalised ground point density. All images within each column bear the same classification. Normalised density: white spots indicate the absence of ground hits. Constant colour palette (0–1 weighted points/m^2).

Table 2. Mean point densities and point cloud structure in the four sample areas.

	Category	Spring 2007		June 2010		May 2011		Nov. 11		June 2012	
		Pt/m^2	%	Pt/m^2	%	Pt/m^2	%	Pt/m^2	%	Pt/m^2	%
Area 1	Ground points	6.2	38	0.3	4	1.3	3	10.9	37	5.6	18
	Last echoes	9.6	59	3.8	55	23.8	58	14.8	50	15.9	50
	All echoes	16.2	100	6.9	100	40.8	100	29.6	100	31.4	100
Area 2	Ground points	8.1	49	0.7	7	4.8	6	21.7	41	7.7	12
	Last echoes	9.8	59	4.4	46	47	58	26.2	49	29.9	48
	All echoes	16.7	100	9.6	100	81.3	100	53.4	100	62.6	100
Area 3	Ground points	7.2	48	0.3	4	2.3	3	17.9	35	1.8	4
	Last echoes	9.7	64	3.6	54	44.9	63	24.2	47	23.1	57
	All echoes	15.1	100	6.7	100	71.3	100	51.2	100	40.2	100
Area 4	Ground points	8.3	53	0.5	7	4	6	14.7	34	3.9	7
	Last echoes	9.9	63	3.8	53	42.8	63	21.2	50	30.1	53
	All echoes	15.8	100	7.2	100	69.3	100	42.8	100	56.8	100
Average	Ground points	7.45	47	0.45	5.5	3.1	4.5	16.3	36.75	4.75	10.25
	Last echoes	9.75	61.25	3.9	52	39.625	60.5	21.6	49	24.75	52
	All echoes	15.95	100	7.6	100	65.675	100	44.25	100	47.75	100

A surprisingly higher percentage of filtered ground points for Area 1, 18%, recorded in June 2012 compared with 4% and 3% for June 2010 and May 2011, respectively, can be explained by the fact that the area had been partially cleared of woodland between November 2011 and June 2012. This can be observed in Figure 11 as a linear pattern of clearance lines, 5 m wide and 20 m apart. While this impacted the archaeological interpretation of the area (see below), no other changes in land use have been recorded between 2007 and 2012.

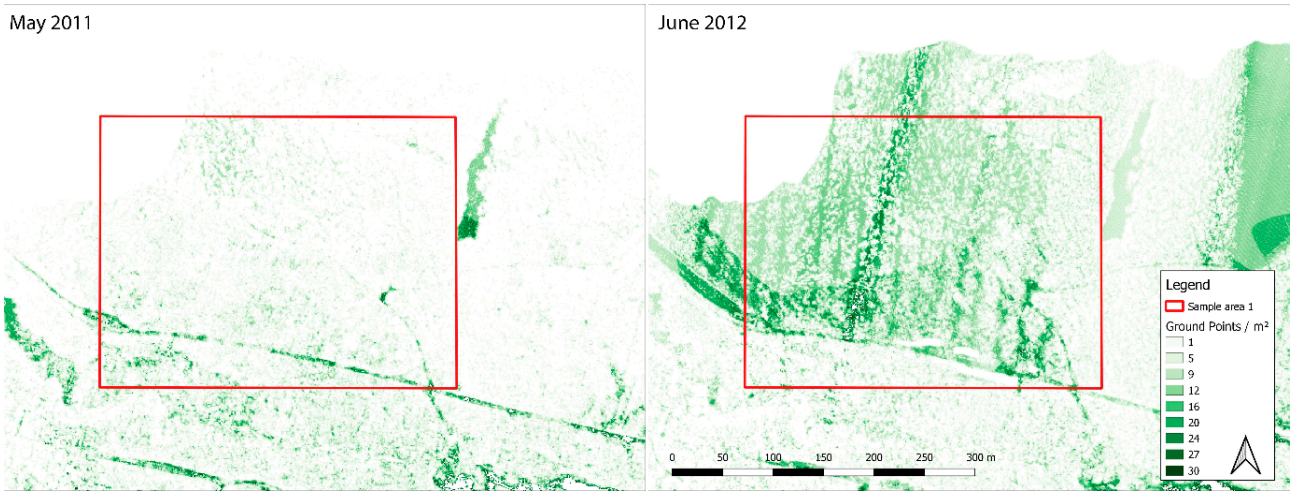

Figure 11. (**Left**): ratio of ground points and total points per m^2 from May 2011 indicating dense vegetation. (**Right**): the same area from June 2012 shows that due to forest management, north-south-oriented 5 m wide lines of trees had been removed. As a result, more ground points could be collected by ALS in the respective area, which is indicated by the darker green tones.

5.2. Interpretation Results

Figures 12–15 illustrate the results of interpretation of five sets of DFM visualisations for the sample areas. The positive openness visualisation (left column) is presented with the outcomes of the "copied interpretation" (middle column) and of the "individual interpretation" (right column). While these two interpretations were undertaken by different authors, the results correspond quite well although they slightly differ in execution. For instance, the linear field boundaries were polygonised by the author of "copied interpretation", while these were mapped as large area features, or a "former field system", in "individual interpretation" (cf. Figure 12, top row).

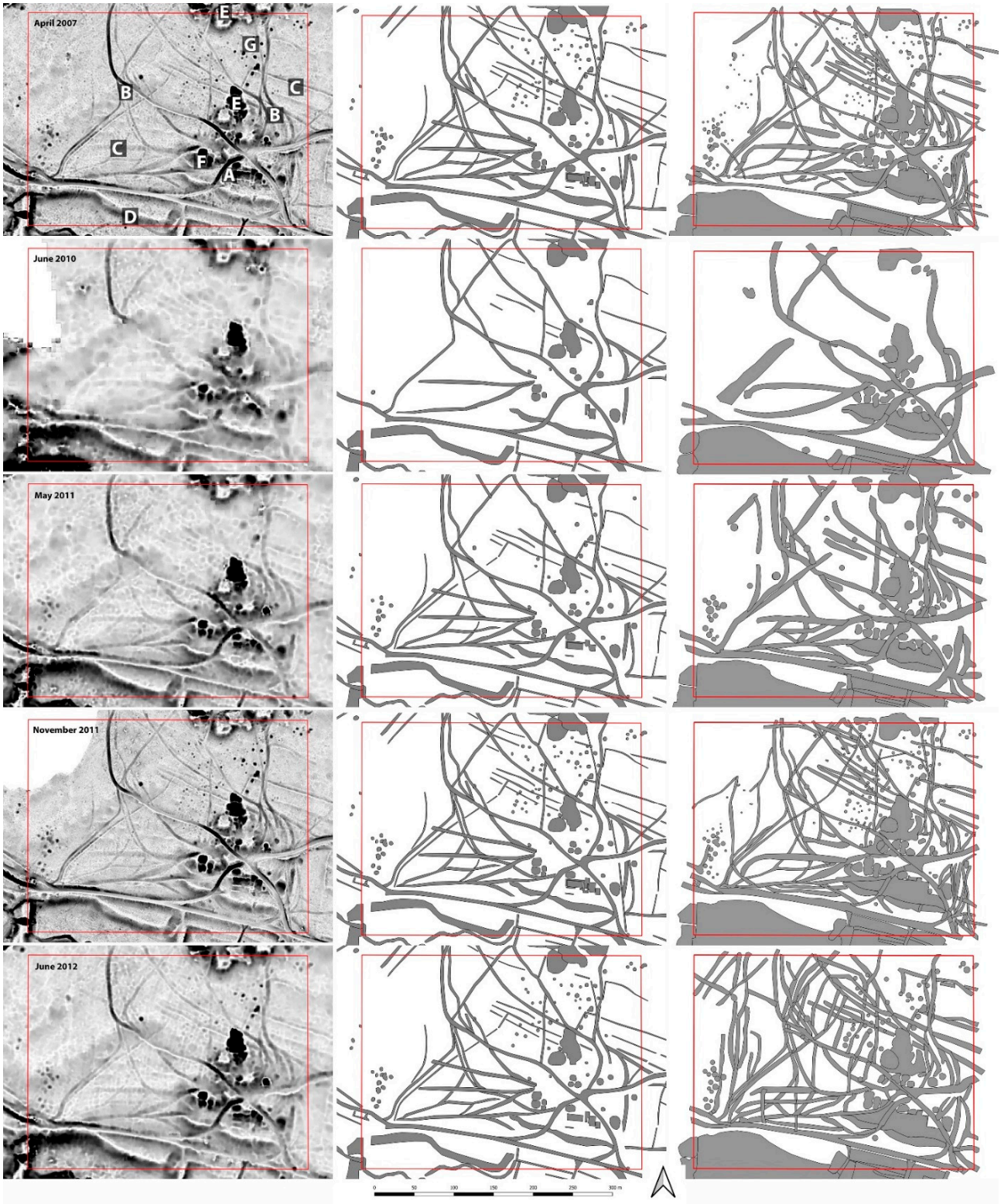

Figure 12. Area 1. The columns represent a visualisation of the dataset using positive openness with colour gradient black to white, stretch to min–max min. 1.41–max. 1.58 (**left**), results of the "copied interpretation" (**centre**), and results of the "individual interpretation" (**right**). The rows correspond to the individual datasets as indicated for each row in the left image. The red box represents the boundary of the sample area. The letters in the upper left image refer to the text.

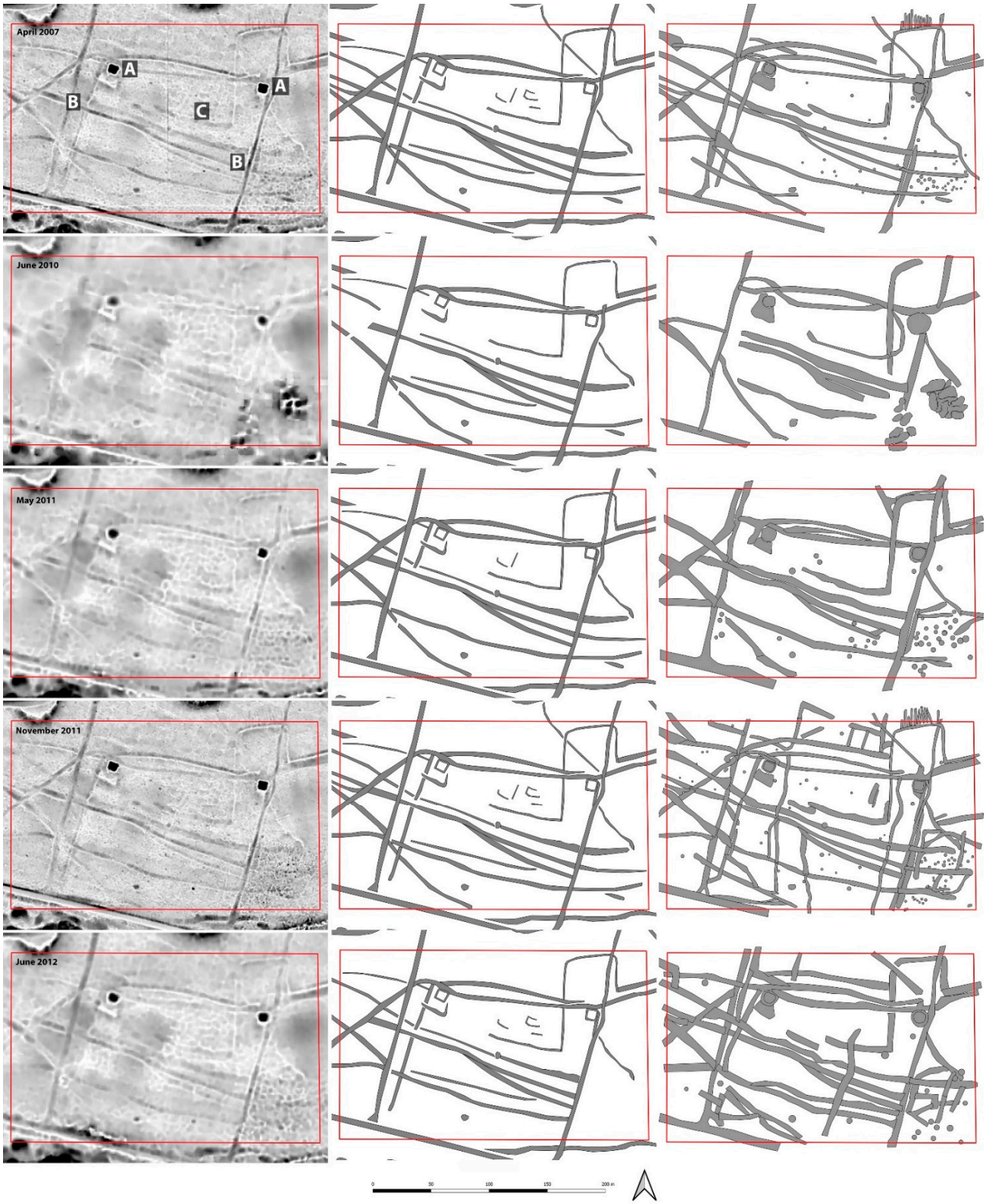

Figure 13. Area 2. The columns represent a visualisation of the dataset using positive openness with colour gradient black to white, stretch to min–max min. 1.41–max. 1.58 (**left**), results of the "copied interpretation" (**centre**), and results of the "individual interpretation" (**right**). The rows correspond to the individual datasets as indicated for each row in the left image. The red box represents the boundary of the sample area. The letters in the upper left image refer to the text.

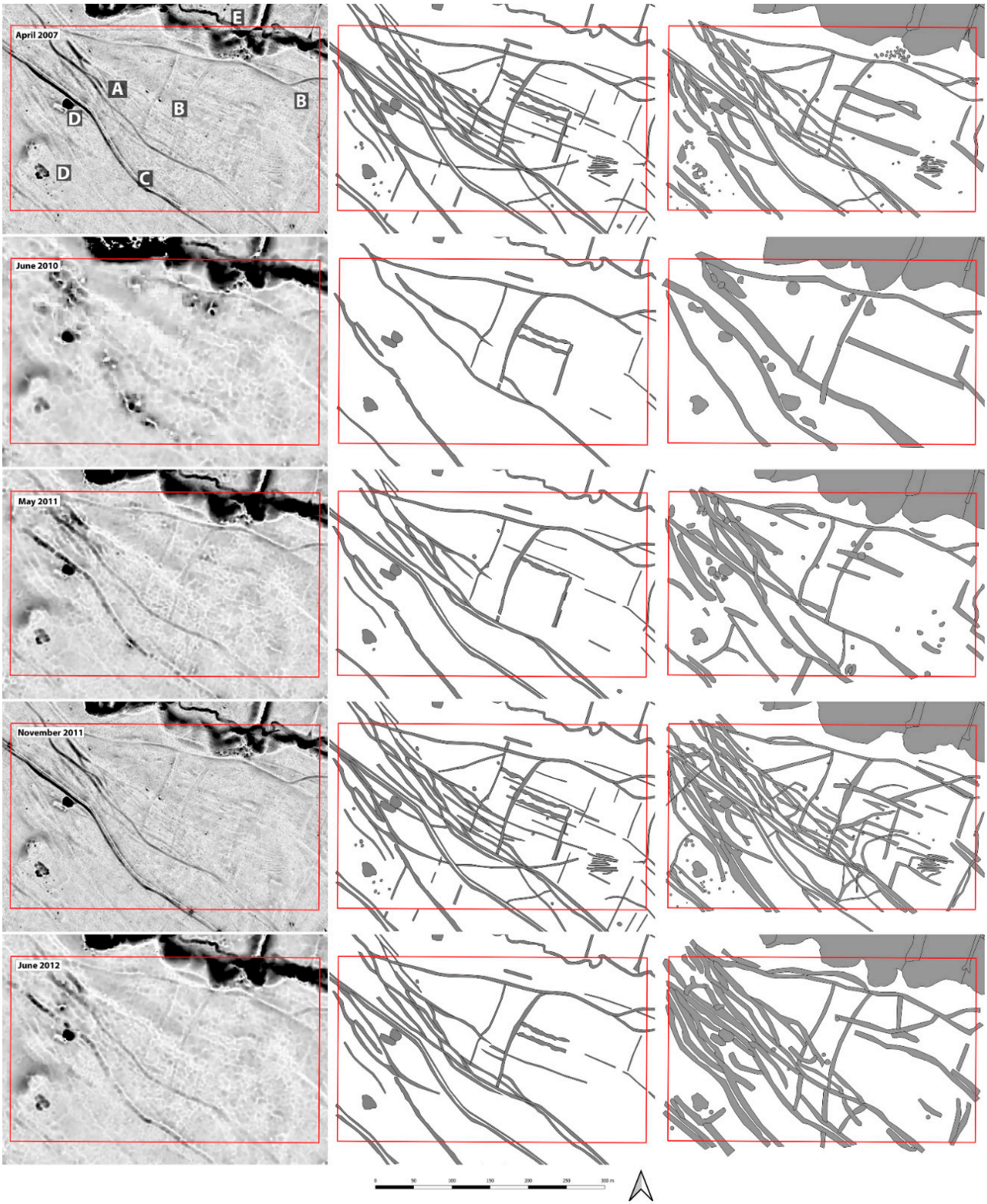

Figure 14. Area 3. The columns represent a visualisation of the dataset using positive openness with colour gradient black to white, stretch to min–max min. 1.41–max. 1.58 (**left**), results of the "copied interpretation" (**centre**), and results of the "individual interpretation" (**right**). The rows correspond to the individual datasets as indicated for each row in the left image. The red box represents the boundary of the sample area. The letters in the upper left image refer to the text.

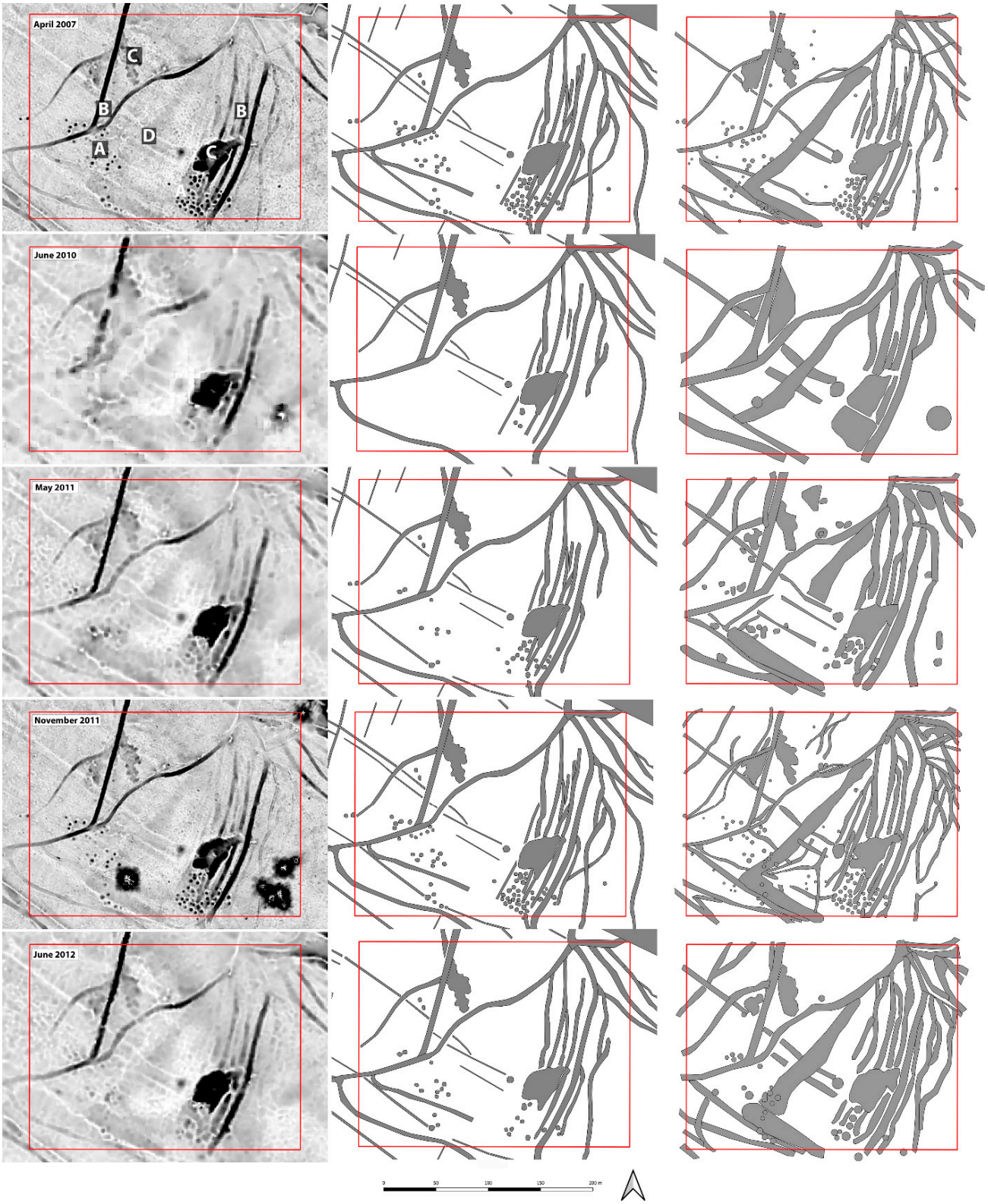

Figure 15. Area 4. The columns represent a visualisation of the dataset using positive openness with colour gradient black to white, stretch to min–max min. 1.41–max. 1.58 (**left**), results of the "copied interpretation" (**centre**), and results of the "individual interpretation" (**right**). The rows correspond to the individual datasets as indicated for each row in the left image. The red box represents the boundary of the sample area. The letters in the upper left image refer to the text.

The archaeological features in Area 1 are associated with a farmstead and disused stone quarries (cf. top left image of Figure 12). The architectural remains of a farm building sit in the SE part of the area (A) and are flanked by many linear structures, including roads and pathways (B), as well as terraces and field boundaries (C). The extensive terraces and fields in the S align with the course of a small river (D). Numerous former stone quarries (E) were identified, together with small round pit-like structures interpreted as limekilns (F) and, following the stratigraphic evidence, bomb craters (G).

The striking features in Area 2 (Figure 13) are the square remains of two stone-built hermits' cells (A) measuring roughly 8 m by 8 m. These are situated within an area of pathways (B) and field boundaries (C), with the latter parallel and perpendicular to the sloping terrain.

Area 3 (Figure 14) comprises numerous linear features. An extensive zone of intersecting hollow ways (A) encroaches on a regular system of shallow ditches (B), the latter interpreted as former field boundaries. The distinct linear feature running NW-SE (C) is formed by an enclosure wall of the friary flanked by a hollow way. Small stone quarries are also present (D) within the higher ground. On the alluvial plain in the NE, dams were constructed to establish fishponds (E).

Area 4 (Figure 15) is rich in round features, (A) interpreted as small quarries, bomb craters and badger setts, as a more detailed archaeological classification is currently not possible and located amongst dense and low vegetation. Some pits intersect and others are cut by hollow ways (B) and two extensive quarries (C). The parallel linear structures running from NW to SE represent field boundaries (D), which predate the hollow ways.

5.3. Quantitative Analysis

The polygons resulting from "individual interpretation" were rasterized to allow for a cell-by-cell comparison. The interpretative mapping, based on Spring 2007 data, was paired with the rasterized outputs of each interpretation of data acquired in the subsequent surveys. Only two categories of objects were considered—linear features and pits and the results of this approach are presented in Table 3 and visualized in Figure 16. The plot indicates that the number of pixels representing archaeological features visible in the reference dataset increases, while the number of pixels representing features visible in both rasters in a pair decreases, aligning with the decreased point density of the second dataset. These observations are discussed in the following section.

Table 3. Results of comparing the Spring 2007 data with the four other sets. The values comprise the sum of raster cells for (i) linear features, (ii) pits, and (iii) for these categories together. Numbers divided by 1000.

	Cell Value	June 2010			May 2011			November 2011			June 2012		
		Linear Features	Pits	Total	Linear Features	Pits	Total	Linear Features	Pits	Total	Linear Features	Pits	Total
Area 1	−1	29.7	2.6	32.4	47.0	7.9	54.9	34.1	3.2	37.3	60.3	4.9	65.3
	1	45.0	9.1	54.2	25.8	6.6	32.3	17.3	3.6	20.9	21.4	5.3	26.7
	2	39.3	7.4	46.8	58.6	10.0	68.6	67.0	13.0	80.0	63.0	11.3	74.2
Area 2	−1	13.6	3.1	16.7	19.1	2.0	21.1	19.7	0.9	20.6	27.5	1.1	28.7
	1	20.2	8.7	21.1	11.5	0.8	12.2	5.3	0.6	6.0	6.8	0.9	7.7
	2	16.8	1.3	16.9	25.5	0.2	25.7	31.6	0.4	32.0	30.1	0.1	30.3
Area 3	−1	28.4	1.9	30.4	31.2	2.3	33.5	42.0	0.7	42.8	60.4	1.5	61.8
	1	49.0	2.7	51.8	37.4	2.6	40.0	18.9	2.1	21.1	25.8	2.6	28.4
	2	28.7	1.5	30.2	40.4	1.6	42.0	58.8	2.1	60.9	51.9	1.6	53.5
Area 4	−1	23.0	6.7	29.7	25.9	6.4	32.4	21.4	1.5	22.9	28.2	3.2	31.3
	1	16.5	4.3	20.8	13.7	4.4	18.1	7.6	2.4	10.0	8.1	3.9	12.0
	2	30.5	7.6	38.1	33.4	7.5	40.9	39.5	9.5	49.0	39.0	8.0	46.9

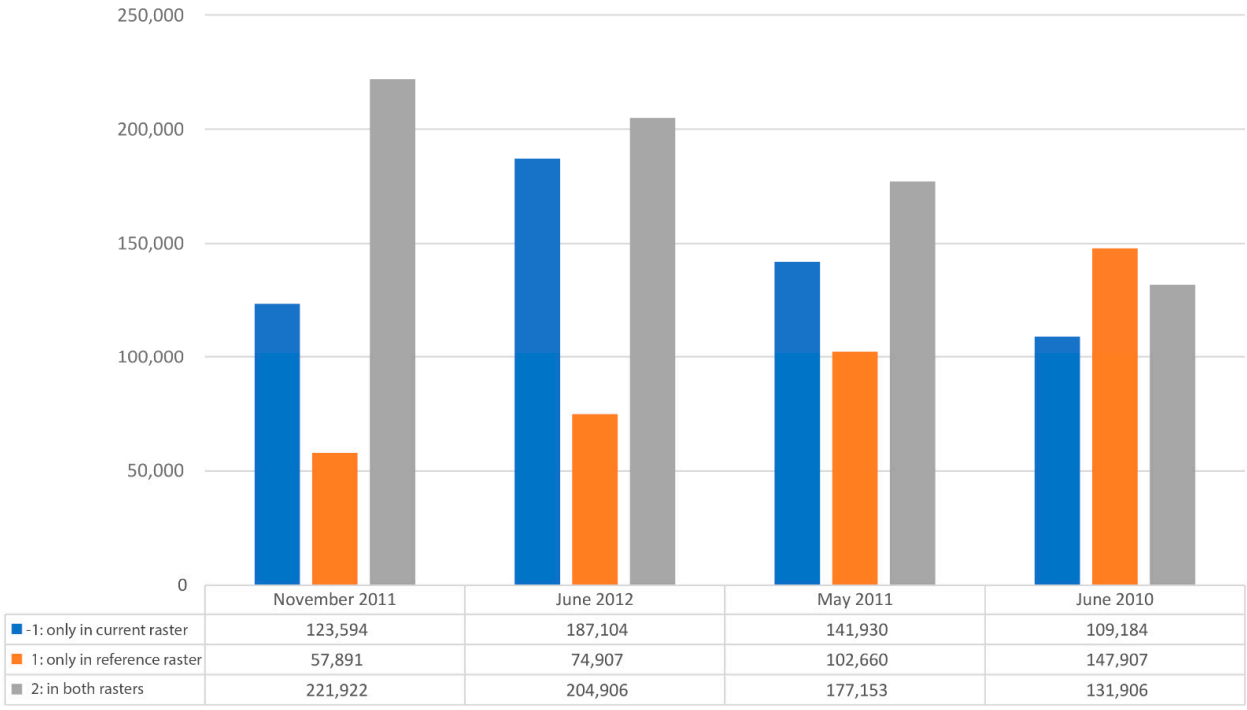

	November 2011	June 2012	May 2011	June 2010
-1: only in current raster	123,594	187,104	141,930	109,184
1: only in reference raster	57,891	74,907	102,660	147,907
2: in both rasters	221,922	204,906	177,153	131,906

Figure 16. Summed up results of mutual comparison of Spring 2007 interpretation and results derived from the other datasets for all sample zones.

The outcomes of the "copied interpretation" are compared in Table 4 and illustrated as a bar plot in Figure 17. The number of archaeological features decreases with the lower ground points density of the dataset (compare Figure 17 with Figure 10). The only exception is the interpretation of Area 1 using the June 2012 data. Here, more archaeological features were identified than expected, which results primarily from the woodland clearance activity in 2011, which thinned the forest and, consequently, a higher number of ground points was recorded (see Figure 11).

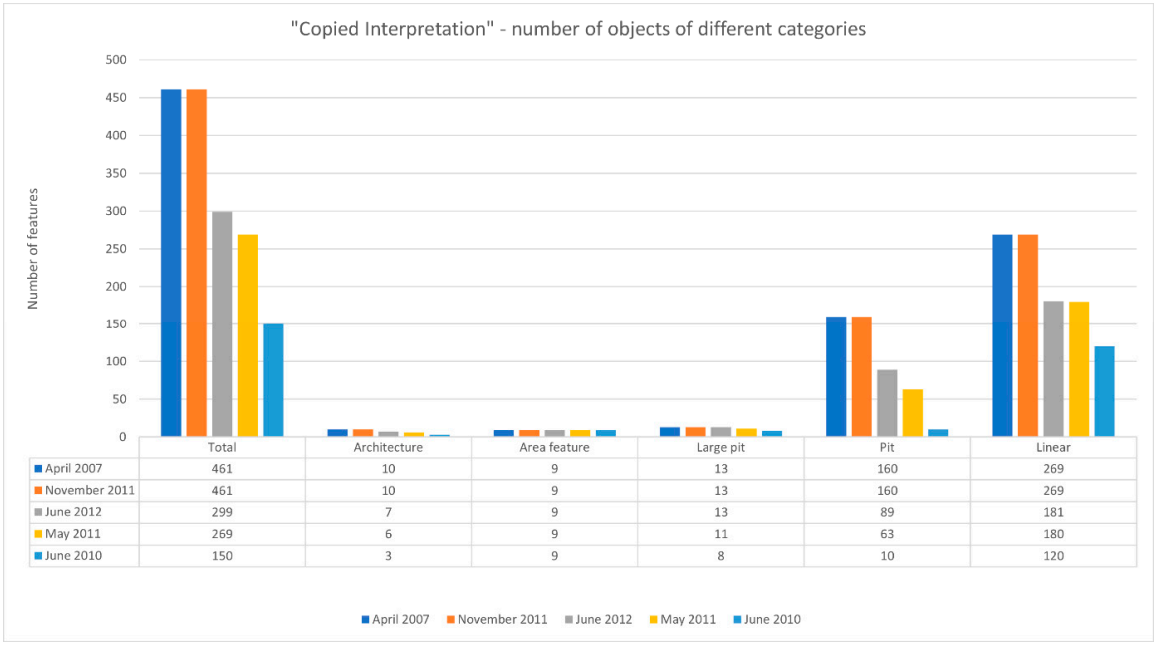

	Total	Architecture	Area feature	Large pit	Pit	Linear
April 2007	461	10	9	13	160	269
November 2011	461	10	9	13	160	269
June 2012	299	7	9	13	89	181
May 2011	269	6	9	11	63	180
June 2010	150	3	9	8	10	120

Figure 17. Number of individual features per category from "copied interpretation" drawings of each dataset.

Table 4. Numbers of individual features from each "copied interpretation" drawing.

	Dataset	Architecture	Area Feature	Large Pit	Pit	Linear	Total
Area 1	2007 April	8	4	12	76	72	172
	2010 June	1	4	7	5	36	53
	2011 May	4	4	10	29	60	107
	2011 November	8	4	12	76	72	172
	2012 June	5	4	12	57	66	144
Area 2	2007 April	2	0	0	2	48	52
	2010 June	2	0	0	2	31	35
	2011 May	2	0	0	2	40	44
	2011 November	2	0	0	2	48	52
	2012 June	2	0	0	2	38	42
Area 3	2007 April	0	3	0	16	105	124
	2010 June	0	3	0	0	24	27
	2011 May	0	3	0	4	47	54
	2011 November	0	3	0	16	105	124
	2012 June	0	3	0	1	47	51
Area 4	2007 April	0	2	1	66	44	113
	2010 June	0	2	1	3	29	35
	2011 May	0	2	1	28	33	64
	2011 November	0	2	1	66	44	113
	2012 June	0	2	1	29	30	62

6. Discussion

6.1. Quantitative Approach

6.1.1. Comparison Based on Cell Values

As to be expected, there is a significant coherence between the two leaf-off datasets from April 2007 and November 2011. In this case, the total number of comparison raster cells representing features detected in both rasters (the "2" value) is the highest in every study area. This means that no other data is as similar to the reference dataset as the Autumn 2011 outcome (compare interpretations from Figures 12–15). This is obviously because both datasets were collected in a similar phase of vegetation conditions (leaf-off). Anyhow, it seems that in early November 2011, fallen leaves had already deflated after some rainfall and therefore did not fill up microtopographic features [compare 11]. The difference in the mapped morphology of features visible in both datasets, due to uneven distribution of ground points, is the primary reason for the small number of 2007 raster only values ("1" in Figure 16).

Figure 16 indicates that number of cells representing features detected in both rasters (value "2") in the Spring 2007/June 2010 pair comprise roughly a half of the cells representing features detected in both rasters in the Spring 2007/November 2011 pair. In the case of the former pair, the number of pixels with cells representing archaeology identified solely in the reference dataset (value "1") is the highest. This suggests that values "1" and "2" are correlated and indicates that many baseline features (identified in Spring 2007 data) were not visible in the data collected over three years later. In addition, if the low total and ground point density of the June 2010 data is considered, this dataset provides the weakest basis for archaeological interpretation.

However, the comparisons between the Spring 2007 data and the outcomes of May 2011 and June 2012 surveys present a more complex picture. The difference between the outputs of interpretative mapping based on May 2011 and June 2012 data is not obvious. The amount of the extracted archaeological information seems to be similar (compare Figures 12–15) and there is a significant proportion of features detected in both rasters (value "2") if these datasets are compared with the reference 2007 data. In fact, the number

of cells with value "2" represent 92% (for Spring 2007/May 2011) and 80% (for Spring 2007/June 2012) of the total cells with the same value identified for the leaf-off pair. At the same time, both leaf-on datasets demonstrate a lower number of 2007 raster only values ("1"), as values "1" and "2" are correlated. This would counterintuitively indicate that the impact of foliage on the detectability of archaeological features is limited and is addressed below.

At the same time, we see a high occurrence of features only detected in the non-reference raster (value "−1") in all datasets indicating that there is a high number of pixels representing archaeological features identified solely in the non-reference datasets (Table 3 and Figure 16). One would rather expect low numbers as the Spring 2007 data show archaeological information quite clearly, but even the low ground point density June 2010 data demonstrate several "−1" values similar to the November 2011 interpretation. However, it is important to note that coarser DFMs resulting from the leaf-on surveys and building on lower ground point density impact the size and shape of relief features, and the qualitative approach addresses this issue below.

6.1.2. Comparison Based on Discrete Features

While the comparison based on cell values proved to be complex, the results of the "copied interpretation" were used to compare the number of individual features visible across the datasets (Table 4 and Figure 17). Here, the changing geometry of a relief feature is not an issue, as only the number of polygons and not their extent is considered.

Table 4 illustrates the visibility of linear, round, and area features due to the change in foliage. All features mapped using the visualisations of Spring 2007 data were identified also in the second leaf-off dataset acquired in November 2011. The interpretation of the data gathered in May and June, however, produced lower numbers of identified features. Both high-density data acquisition campaigns of May 2011 and June 2012 reveal roughly two thirds of the linear features and between 39% and 59% of small pits visible in the reference dataset. The June 2010 data shows less than half of the baseline linear features and only 6% of the pits. While other features, including architectural remains, area features and large pits, are statistically insignificant to be compared individually, the total number of features identified in the compared leaf-on datasets varies from 33% for June 2010 to 58% for May 2011 and 65% for June 2012 data.

The wood clearance in Area 1 discussed above resulted in a deviation that made 92% of the baseline linear features and 75% of the baseline small pits visible in the June 2012 data, whereas 83% and only 38% of the respective features were identified in the May 2011 data (Table 4). The number of small pits recorded in Area 1 through the later high-density leaf-on survey nearly doubled when compared with the outcomes of a similar survey undertaken before the clearance. While the comparable number of pits identified in Area 4 (28 for May 2011 and 29 for June 2012) demonstrates that these two datasets are generally similar, the local increase in ground point density due to tree clearance causes the higher success rate recorded for June 2012 data and, as such, it should be taken with caution.

It is worth noting that this approach results from a particular decision made for the purposes of this study and it relies on the availability of a high-quality reference data. Features identified in the 2007 dataset fed the interpretation of subsequent DFMs. If the visualisations of June and July data were interpreted from scratch (cf. "individual interpretation" approach), it is very likely that some features might have been omitted and the number of visible features would have been lower.

6.2. Qualitative Approach

Although the quantitative approach presents some aspects of information loss which corresponds with the varied characteristics of the ground point distribution, a detailed understanding of such changes may only be achieved through a qualitative comparison. The raster cell-based approach returned a rather high number of features detected either in both rasters or in the non-reference datasets ("2" and "−1" values—Table 3 and Figure 16)

suggesting that a reduced ground point density produces more archaeologically relevant pixels than the reference dataset. This approach, however, does not provide a reason for this unexpected increase of archaeologically relevant pixels. Therefore, in the following, we use the four sample zones to discuss changes in morphology of linear and pit-like features throughout different datasets.

Figure 18 presents a part of Area 1 with the remains of a ruined farm building occupying a terrace covered with deciduous trees of varying height and understory. The low vegetation is confined to nettles which can reach 1 m in height in June. The ruined building is clearly visible in the leaf-off datasets and individual walls and compartments with at least one entrance can be mapped. While the building is still identifiable in the May 2011 and June 2012 data, the detail is lost, and the structure is hardly visible in the June 2010 data. Indeed, both foliated trees and nettles covering the area contribute to the "fuzziness" observed in the leaf-on datasets and it is difficult to measure the impact each forest layer has on survey outputs. Wild garlic, present during the Spring 2007 campaign, had no effect on the recording of archaeological relief features. The detail observed in this dataset is almost identical to the results of the November 2011 survey.

In this low-density dataset, only the artificial terrace on which the ruined farmhouse is located and two hollow ways are discernible. The "copied interpretation", which distinguished individual compartments of the building and the terrace demonstrates a reduction in visibility of archaeological features with the change in ground point density (compare Figure 12). The area-based "individual interpretation" focused on the artificial terrace and this large feature is visible in all ALS datasets. Hollow ways and a modern gravel road, as well as large pits of lime kilns, can also be identified in all terrain models, even if their shape is less obvious in the June 2010 data.

A similar situation is presented in Figure 19. A hermit's cell, roughly 8 m by 8 m, located in an area of mixed trees and infrequent shrubs can be observed in detail using the March/April and November datasets. Its shape and the thickness of the foundation wall can be mapped accurately in the leaf-off data. While the structure is visible in all datasets, the detail is lost in the leaf-on datasets; the less ground points, the more it resembles a big roundish sunken feature. The trapezoidal terrace, however, remains visible and maintains its shape (compare Figure 13).

The third example presents a part of the network of hollow ways in Area 3 (Figure 20). While many of the tracks were recorded at the peak of the vegetation season, the shallow features are no longer visible and only deeper incised hollow ways are revealed. The very few hollow ways that are visible in the June 2010 data seem to be much wider than the same features in other datasets. Parallel lines running close to each other seem to form a single, wide path (compare Figure 14) in this low-density data. As a result, many "−1" values were recorded in the raster-based comparison. In addition, several mound-like features occur, resulting from erroneous ground point classification. Such false positives were identified as real features in the "individual interpretation", and thus also contributed to the high number of "−1" values.

The final example is overgrown by dense low vegetation and presented in Figure 21. Individual pits measuring up to three metres in diameter and 10 cm to 70 cm deep, are clearly visible in the March/April and November data. While the pattern they create is visible in the high-density data from May 2011 and June 2012, a smaller number of pits can be identified and those recorded seem to be considerably larger. Again, this is due to the reduced number of ground points, as points within neighbouring pits were interpolated to form larger structures. Therefore, the "individual interpretation" correctly identified the pits, but the number, shape and size of the mapped features is notably different. In the June 2010 data, pits seem to have almost completely dissolved, giving only an impression of an undulating area. Such growth in the size of features, resulting from "individual interpretation" (compare Figure 15), contributed to the high number of values detected either in both rasters or in the non-reference datasets ("2" and "−1" values) in the raster-based approach. While the clustering of pits causes that these features are visible in May

2011 and June 2012 data, isolated pits, e.g., in the W part of Area 4, are obscured and do not show in the leaf-on datasets (Figure 21).

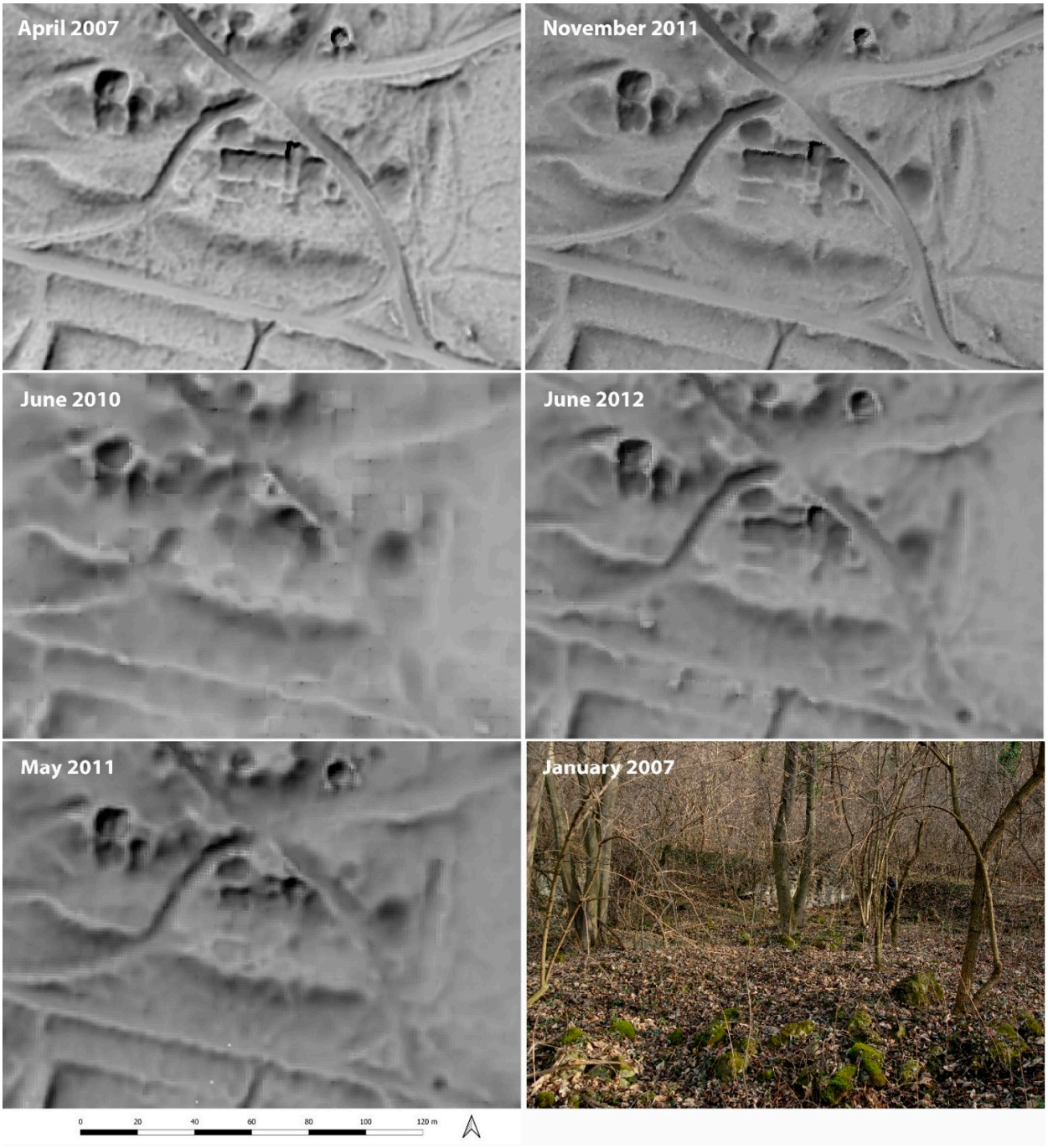

Figure 18. Sample zone from Area 1 displaying a ruined farm building. All visualizations are a combination of positive openness (with colour gradient black to white, stretch to min–max, min. 1.41–max. 1.58) and hillshade. The photograph (lower right image) shows the area of the farm building from January 2007 (photograph by M. Doneus).

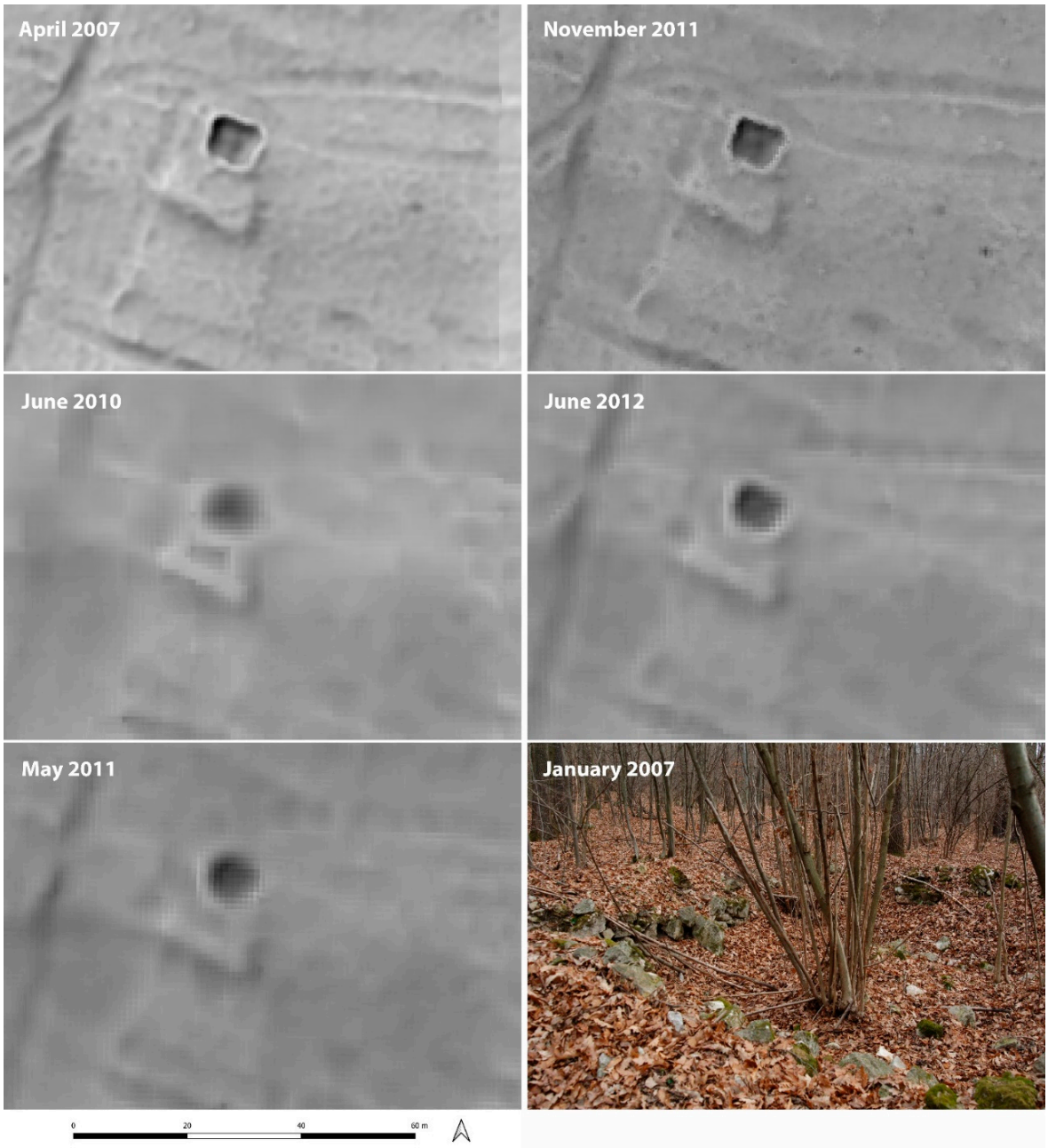

Figure 19. Sub-sample of Area 2 displaying the foundation of a hermit's cell on a small artificial terrace. All visualizations are a combination of positive openness (with colour gradient black to white, stretch to min–max, min. 1.41–max. 1.58) and hillshade. The photograph (**lower right image**) shows the area of the farm building from January 2007 (photograph by M. Doneus).

6.3. The Visibility of Archaeological Features

Our study demonstrates that ground point density is one of the key factors to be considered in archaeological application of ALS, and this corresponds with the results of other studies (e.g., [49]). It is worth noting that while the high-density lidar surveys in leaf-on conditions can produce some satisfactory data, the vegetation has a significant impact on the visibility of archaeological features. The high-quality November 2011 data, which was collected with the same equipment and flight parameters as the surveys undertaken in May 2011 and June 2012 (compare Tables 1 and 2), recorded a mean density of 4.4 ground points and 13.1 last echoes per m^2, i.e., a ratio of 34%. Such ratio for the May 2011 and June 2012 surveys is at 7% and 15%, respectively. Incidentally, at 15.1 points per m^2, the mean

last echo density for the latter survey was notably lower than that recorded in the former campaign (22.8 pts/m^2). The higher percentage of last echoes representing ground points in June 2012 data resulted from a 34% decrease in the mean last echo density if compared with May 2011 data, which can be explained primarily through the wood clearance that thinned the canopy before the final survey took place. Therefore, the impact of vegetation is clearly visible if the May 2011 data is compared with the outputs of the November 2011 survey. The former recorded significantly higher mean last echo density, at 22.8 pts/m^2, with 13.1 pts/m^2 for the latter survey. This increase of 174% is contradicted by the mean ground point density, at 1.5 pts/m^2 and 4.4 pts/m^2 respectively, demonstrating a decrease of 66%. Thus, this comparison demonstrates that the impact of vegetation cannot be easily compensated through increasing the total point density of an airborne lidar survey.

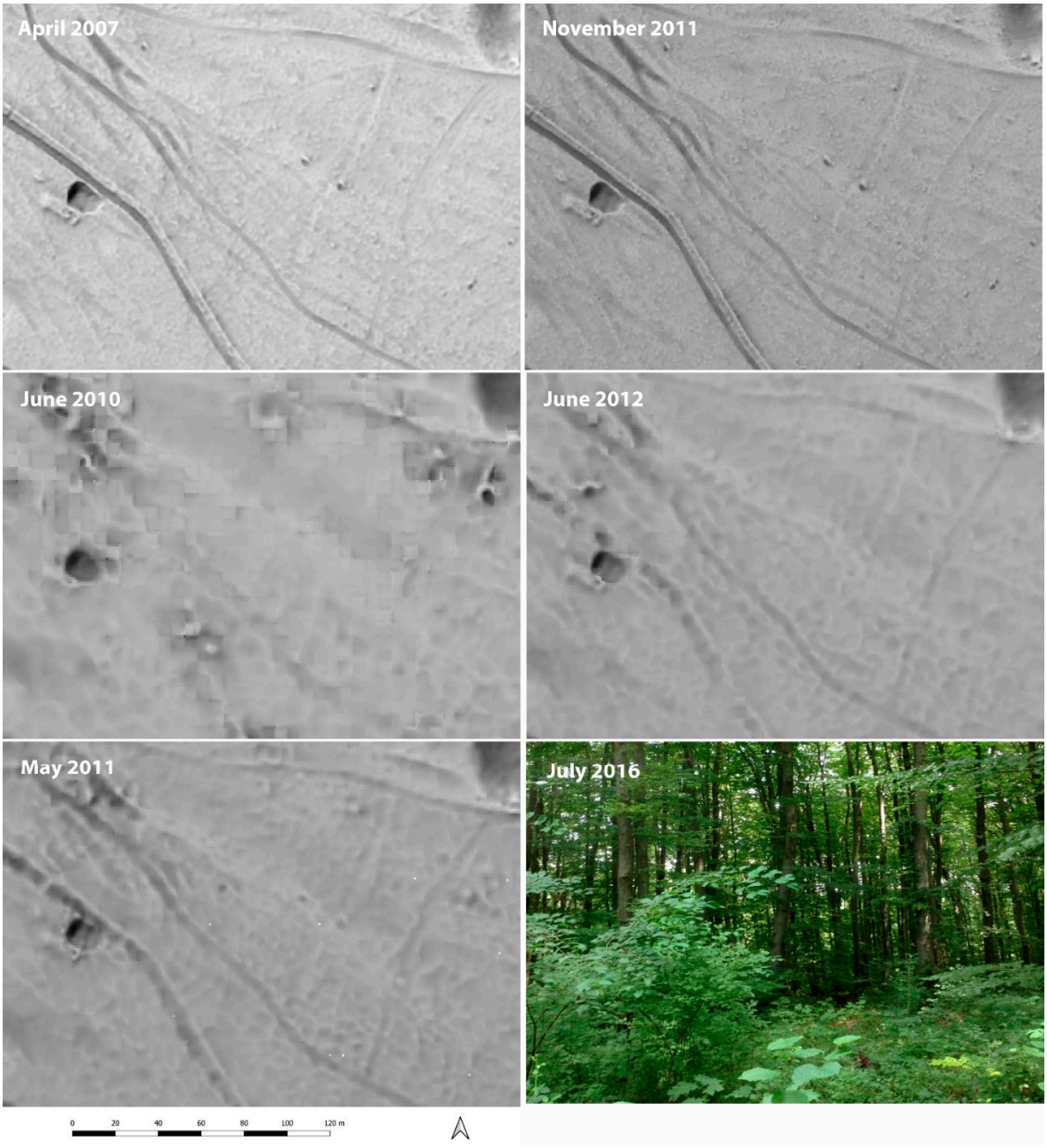

Figure 20. Part of a network of hollow ways in Area 3. All visualizations are a combination of positive openness (with colour gradient black to white, stretch to min–max, min. 1.41–max. 1.58) and hillshade (photograph by Ł. Banaszek).

Figure 21. Sub-sample of Area 4. All visualizations are a combination of positive openness (with colour gradient black to white, stretch to min–max, min. 1.41–max. 1.58) and hillshade. The photograph (**lower right image**) shows the area from January 2007 (photograph by M. Doneus).

It must be mentioned that our statements may be only applicable to areas of temperate forest. In areas with extremely dense vegetation (e.g., rainforest, macchia shrubland) higher point densities might not necessarily result in more ground points. Nevertheless, our study seems to align with the outcomes of a survey in the rainforest, which has not only demonstrated that ground point density is a very important factor, but also suggested the use of lower pulse repetition frequency to allow for higher energy per pulse and, consequently, a higher penetration rate [6]. This indicates that our results seem to have a broader application than just for the forested areas of Central Europe. The suggestion of Fernandez-Diaz et al. is also reflected in the outcomes of the Spring 2007 data, in which the figure for mean ground point density comprises 56% of mean last echoes density. Thus, a higher ground point density and the ratio of mean ground point density divided by last

echoes was recorded for the lower pulse repetition frequency Spring 2007 data than for the November 2011 data, despite the latter recording a 3.4 pts/m^2 higher mean last echoes density than the former. Nonetheless, beside different pulse repetition frequency, other reasons including variability in flight speed, difference in scan angle and residual autumnal vegetation must also be considered.

It is evident that the detail of archaeological information decreases with the reduced lidar surface sampling, i.e., a smaller number of ground points recorded. Over 50% of the baseline archaeological features were identified in the high-density data collected in May 2011 and June 2012 through the object-based comparison of the "copied interpretation". In contrast, the decreased ground point density, caused by leaf-on conditions, impacts the appearance, size and shape of the recorded relief features. Parallel hollow ways and closely spaced pits merged to form large features and produced a high number of values detected either in both rasters or in the non-reference datasets ("2" and "−1" values) in the raster cell-based comparison. At the same time, small and isolated features were obscured, and false positives were produced due to the random distribution of ground points. These false positive features are found in the "individual interpretation" of the leaf-on times and are on the one hand virtually generated objects (mainly discrete features, e.g., Figure 13, May and June, Figure 14, May), on the other hand they can be actual features that have changed appearance (Figure 15, May). In the latter case, linear structures are also affected. Therefore, caution should be exercised when interpreting data sets with low and unevenly distributed ground point density. Nonetheless, it is surprising that over two thirds of the baseline linear archaeological features were identified in both high-density leaf-on datasets, although it has been acknowledged that this success rate would potentially be lower if no reference data were available. The visibility of shallow round structures is the most affected by the change in ground point density.

Our study demonstrates clearly that leaf-on conditions produce lower ground point density, but the applied methodology does not allow for differentiating and quantifying this impact for each forest layer, for instance foliated trees and nettles. The latter, which often reach over 1 m in height, might be a major factor in the "fuzzy" appearance of relief features in Area 1. This is in opposition to the extremely low vegetation, such as wild garlic, which was observed at the time of the Spring 2007 survey. This herbaceous plant had no effect on the detection and detail of archaeological structures. While the DFM derived from November 2011 data demonstrates similar detail to the reference March/April 2007 dataset, there is some noise in the former that can be attributed to a denser vegetation, which possibly included leaves on trees and shrubs as well as patches of rotting understorey. This produced some archaeological non-features, "−1" value, in cell-based comparison. Nonetheless, the "copied interpretation" identified 100% of baseline features in the autumnal data.

The low-density survey of June 2010 delivered the poorest results and produced a reduced number of features presenting significant change in size and shape. The fall in ground point density can be observed from 5.4 (Spring 2007) to 4.4 (November 2011), 2.2 (June 2012), 1.5 (May 2011) and 0.5 (June 2010). The associated increased fuzziness of archaeological features, as well as the decreased detection rate as seen from the "copied interpretation" seem to align with the results of a study in the boreal forest. There, the authors argue that the mean ground point density of about 5 pts/m^2 is sufficient to identify vast majority of archaeological features [50]. While such point density comprises a threshold below which the detectability of archaeological features falls notably overall, a denser point cloud can help to investigate the details of the recorded features. The use of UAV-based laser scanners may prove helpful, at least when surveying small areas with dense vegetation [49,51–53].

7. Conclusions

This paper foregrounded some considerations concerning the data acquisition and general applicability of ALS datasets for archaeological purposes. In the area of St. Anna

in der Wüste, which contains abundant archaeological traces in relief, five ALS data acquisition campaigns were realized in both leaf-off (April 2007 and November 2011) and leaf-on conditions (May 2011, June 2010 and June 2012).

We have demonstrated that the leaf-on conditions have a significant impact on the readability of archaeological features. The potential to record and recognize such remains is—besides their character (linear or discrete features)—mainly related to the distribution of ground points, which in turn is dependent on the vertical and horizontal structure of the forest. As a result, datasets acquired during the peak of vegetation vigour are characterised by a limited number of ground hits even though the total point densities were significant. The impact of vegetation therefore cannot be easily compensated through increasing the total point density. It is rather the use of a lower pulse repetition frequency with associated higher energy per pulse that seems to have a positive effect in dense vegetation. This clearly confirms the results of other methodological ALS studies; at the same time, it meets the typical expectations and archaeological assumptions.

However, the assessment of the character of the information gain and loss is not straightforward. Based on our dataset comparison, we have demonstrated that particular features become invisible, whilst the morphology of others might be considerably altered. In many cases, low ground point densities blurred the course of linear features. Moreover, clusters of small pits can be aggregated and thus misinterpreted. Although the dimensions of particular features may expand due to the decline in ground point density, the count of recognizable features decreases. However, a mere quantitative approach based on cell counts failed to explain this gain and loss of archaeological information across datasets. This understanding was only achievable via either a quantitative approach based on feature count or a qualitative comparison.

It has been illustrated how leaf-on conditions could lead to altered feature morphology which, in turn, significantly can influence the archaeological interpretation. On several occasions, even false positives were produced. This should be considered when interpreting data sets with low and unevenly distributed ground point density. Nevertheless, those leaf-on datasets should not be totally discarded. Many remains were still identified in those data, which highlights that ALS campaigns during less-than-ideal vegetational conditions or acquired for non-archaeological purposes, like forestry, might still be suitable in specific environments or for answering particular archaeological questions. While the impact of a reduced ground point density will be felt more strongly where highly detailed interpretation is sought, it will be less problematic in large area rapid mapping based on, for example, polygons. Nevertheless, it is advantageous not to rely on data already processed for non-archaeological purposes, but to use, if possible, raw data that can be processed and whose parameters can thus be controlled. This would in any case have a positive effect on the archaeological interpretation. The key issue is that the potential impacts of these factors on archaeological outcomes, specifically the variability in observable detail and its impact on interpretation, are clearly understood.

Author Contributions: M.D.: conceptualization, project administration, data curation (archaeological interpretation—"copied interpretation", statistics), investigation, methodology, software, visualization, writing—original draft. Ł.B.: conceptualization, methodology, data curation (archaeological interpretation—"individual interpretation", data processing, spatial analyses, statistics), writing—methodology, discussion, visualization. G.J.V.: conceptualization, writing—conclusions, review and editing, visualization. All authors have read and agreed to the published version of the manuscript.

Funding: Open Access Funding by the University of Vienna. The research was partly carried out with the financial support of the Austrian Science Fund (FWF): P18674-G02. The contribution of Ł. Banaszek was sponsored by Polish Ministry of Science and Higher Education through the Mobility Plus program (Agreement 1088/MOB/2013/0).

Institutional Review Board Statement: Not applicable.

Informed Consent Statement: Not applicable.

Acknowledgments: The authors thank Christian Briese (EODC) for processing and filtering the datasets, Christian Eberhöfer (Department of Geodesy and Geoinformation, Technische Universität Wien) for providing calculations of the point density maps and Dave Cowley (Historic Environment Scotland) for his valuable feedback. The Ludwig Boltzmann Institute for Archaeological Prospection and Virtual Archaeology (archpro.lbg.ac.at—last access: 6 January 2022) is based on an international cooperation of the Ludwig Boltzmann Gesellschaft (A), Amt der Niederösterreichischen Landesregierung (A), University of Vienna (A), TU Wien (A), University for Continuing Education Krems (A), ZAMG—Central Institute for Meteorology and Geodynamics (A), Spanish Riding School (A), 7reasons (A), LWL—Federal state archaeology of Westphalia-Lippe (D), NIKU—Norwegian Institute for Cultural Heritage (N) and Vestfold fylkeskommune—Kulturarv (N).

Conflicts of Interest: The authors declare no conflict of interest.

References

1. Doneus, M.; Briese, C. Digital terrain modelling for archaeological interpretation within forested areas using full-waveform laserscanning. In Proceedings of the 7th International Symposium on Virtual Reality, Archaeology and Cultural Heritage VAST, Nicosia, Cyprus, 30 October–4 November 2006; Ioannides, M., Arnold, D., Niccolucci, F., Mania, K., Eds.; pp. 155–162.
2. Risbøl, O.; Gjertsen, K.A.; Skare, K. Airborne laser scanning of cultural remains in forests: Some preliminary results from a Norwegian project. In *From Space to Place: 2. International Conference on Remote Sensing in Archaeology: Proceedings of the 2. International Workshop, CNR, Rome, Italy, 2–4 December 2006*; Campana, S., Forte, M., Eds.; BAR International Series S1568; Archaeopress: Oxford, UK, 2006; pp. 107–112. ISBN 1 84171 998 6.
3. Challis, K. Airborne laser altimetry in alluviated landscapes. *Archaeol. Prospect.* **2006**, *13*, 103–127. [CrossRef]
4. Crutchley, S. Light detection and ranging (lidar) in the Witham Valley, Lincolnshire: An assessment of new remote sensing techniques. *Archaeol. Prospect.* **2006**, *13*, 251–257. [CrossRef]
5. Crow, P.; Benham, S.; Devereux, B.; Amable, G. Woodland vegetation and its implications for archaeological survey using LiDAR. *For. Int. J. For. Res.* **2007**, *80*, 241–252. [CrossRef]
6. Fernandez-Diaz, J.C.; Carter, W.E.; Shrestha, R.L.; Glennie, C.L. Now You See It . . . Now You Don't: Understanding Airborne Mapping LiDAR Collection and Data Product Generation for Archaeological Research in Mesoamerica. *Remote Sens.* **2014**, *6*, 9951–10001. [CrossRef]
7. Lozić, E.; Štular, B. Documentation of Archaeology-Specific Workflow for Airborne LiDAR Data Processing. *Geosciences* **2021**, *11*, 26. [CrossRef]
8. Bofinger, J.; Hesse, R. As far as the laser can reach . . . Laminar analysis of LiDAR detected structures as a powerful instrument for archaeological heritage management in Baden-Württemberg, Germany. In *Remote Sensing for Archaeological Heritage Management: Proceedings of the 11th EAC Heritage Management Symposium, Reykjavik, Iceland, 25–27 March 2010*; Cowley, D., Ed.; Archaeolingua, EAC: Budapest, Hungary, 2011; pp. 161–171. ISBN 978-963-9911-20-8.
9. Wroniecki, P.; Jaworski, M.; Kostyrko, M. Exploring free LiDAR derivatives. A user's perspective on the potential of readily available resources in Poland. *Archaeol. Pol.* **2015**, *53*, 612–616.
10. Banaszek, Ł.; Cowley, D.C.; Middleton, M. Towards National Archaeological Mapping. Assessing Source Data and Methodology—A Case Study from Scotland. *Geosciences* **2018**, *8*, 272. [CrossRef]
11. Doneus, M.; Briese, C. Airborne Laser Scanning in Forested Areas—Potential and Limitations of an Archaeological Prospection Technique. In *Remote Sensing for Archaeological Heritage Management: Proceedings of the 11th EAC Heritage Management Symposium, Reykjavik, Iceland, 25–27 March 2010*; Cowley, D., Ed.; Archaeolingua, EAC: Budapest, Hungary, 2011; pp. 53–76. ISBN 978-963-9911-20-8.
12. Banaszek, Ł. *Przeszłe Krajobrazy w Chmurze Punktów*; Wydawnictwo Naukowe UAM: Poznań, Poland, 2015.
13. Klimczyk, A.; Doneus, M.; Briese, C.; Pfeifer, N. Evaluation of different software packages for ALS filtering. In *Archaeological Prospection: Proceedings of the 10th International Conference–Vienna*; Neubauer, W., Trinks, I., Salisbury, R.B., Einwögerer, C., Eds.; Verl. der Österr. Akad. d. Wiss.: Wien, Austria, 2013; pp. 363–366. ISBN 9783700174592.
14. Kiarszys, G.; Szalast, G. Archeologia w chmurze punktów. Porównanie rezultatów filtracji i klasyfikacji gruntu w projekcie ISOK z wynikami opracowanymi w oprogramowaniu LAStools i Terrasolid. *Folia Praehist. Posnaniensia* **2014**, *19*, 267–292. [CrossRef]
15. Banaszek, Ł. Lotniczy skaning laserowy w polskiej archeologii. Czy w pełni wykorzystywany jest potencjał prospekcyjny metody? *Folia Praehist. Posnaniensia* **2014**, *19*, 207. [CrossRef]
16. Štular, B.; Lozić, E. Comparison of Filters for Archaeology-Specific Ground Extraction from Airborne LiDAR Point Clouds. *Remote Sens.* **2020**, *12*, 3025. [CrossRef]
17. Doneus, M.; Mandlburger, G.; Doneus, N. Archaeological Ground Point Filtering of Airborne Laser Scan Derived Point-Clouds in a Difficult Mediterranean Environment. *J. Comput. Appl. Archaeol.* **2020**, *3*, 92–108. [CrossRef]
18. Štular, B.; Lozić, E.; Eichert, S. Airborne LiDAR-Derived Digital Elevation Model for Archaeology. *Remote Sens.* **2021**, *13*, 1855. [CrossRef]
19. Challis, K.; Forlin, P.; Kincey, M. A Generic Toolkit for the Visualization of Archaeological Features on Airborne LiDAR Elevation Data. *Archaeol. Prospect.* **2011**, *18*, 279–289. [CrossRef]

20. Bennett, R.; Welham, K.; Hill, R.A.; Ford, A. A Comparison of Visualization Techniques for Models Created from Airborne Laser Scanned Data. *Archaeol. Prospect.* **2012**, *19*, 41–48. [CrossRef]
21. Kokalj, Ž.; Somrak, M. Why Not a Single Image? Combining Visualizations to Facilitate Fieldwork and On-Screen Mapping. *Remote. Sens.* **2019**, *11*, 747. [CrossRef]
22. Kokalj, Ž.; Zakšek, K.; Oštir, K.; Pehani, P.; Čotar, K.; Somrak, M. *Relief Visualization Toolbox (RVT)*; Institute of Anthropological and Spatial Studies, ZRCSAZU: Ljubljana, Slovenia, 2020.
23. Bradford, J. *Ancient Landscapes: Studies in Field Archaeology*; Bell & Sons: London, UK, 1957.
24. Rączkowski, W. Theoretical dialogues–is there any theory in aerial archaeology? *AARGNews* **2005**, *1*, 12–22.
25. Palmer, R. Knowledge-based aerial image interpretation. In *Remote Sensing for Archaeological Heritage Management: Proceedings of the 11th EAC Heritage Management Symposium, Reykjavik, Iceland, 25–27 March 2010*; Cowley, D., Ed.; Archaeolingua, EAC: Budapest, Hungary, 2011; pp. 283–291. ISBN 978-963-9911-20-8.
26. Palmer, R. Reading aerial images. In *Interpreting Archaeological Topography: Airborne Laser Scanning, 3D Data and Ground Observation*; Opitz, R.S., Cowley, D., Eds.; Oxbow Books: Oxford, UK, 2013; pp. 76–87. ISBN 978-1-84217-516-3.
27. Štular, B.; Eichert, S.; Lozić, E. Airborne LiDAR Point Cloud Processing for Archaeology. Pipeline and QGIS Toolbox. *Remote Sens.* **2021**, *13*, 3225. [CrossRef]
28. White, J.C.; Arnett, J.T.; Wulder, M.A.; Tompalski, P.; Coops, N.C. Evaluating the impact of leaf-on and leaf-off airborne laser scanning data on the estimation of forest inventory attributes with the area-based approach. *Can. J. For. Res.* **2015**, *45*, 1498–1513. [CrossRef]
29. Banaszek, Ł. *The Past Amidst the Woods. The Post-Medieval Landscape of Polanów*; Ad Rem: Poznań, Poland, 2019; ISBN 978-83-916342-6-4.
30. Banaszek, Ł. It takes all kinds of trees to make a forest. Using historic maps and forestry data to inform airborne laser scanning based archaeological prospection in woodland. *Archaeol. Prospect.* **2020**, *27*, 377–392. [CrossRef]
31. Chase, A.F.; Chase, D.Z.; Weishampel, J.F. Lasers in the Jungle: Airborne sensors reveal a vast Maya landscape. *Archaeology* **2010**, *63*, 27–29.
32. Chase, A.F.; Chase, D.Z.; Weishampel, J.F.; Drake, J.B.; Shrestha, R.L.; Slatton, K.C.; Awe, J.J.; Carter, W.E. Airborne LiDAR, archaeology, and the ancient Maya landscape at Caracol, Belize. *J. Archaeol. Sci.* **2011**, *38*, 387–398. [CrossRef]
33. Chase, A.F.; Chase, D.Z.; Fisher, C.T.; Leisz, S.J.; Weishampel, J.F. Geospatial revolution and remote sensing LiDAR in Mesoamerican archaeology. *Proc. Natl. Acad. Sci. USA* **2012**, *109*, 12916–12921. [CrossRef]
34. Beach, T.; Luzzadder-Beach, S.; Krause, S.; Guderjan, T.; Valdez, F.; Fernandez-Diaz, J.C.; Eshleman, S.; Doyle, C. Ancient Maya wetland fields revealed under tropical forest canopy from laser scanning and multiproxy evidence. *Proc. Natl. Acad. Sci. USA* **2019**, *116*, 21469–21477. [CrossRef]
35. Chevance, J.-B.; Evans, D.; Hofer, N.; Sakhoeun, S.; Chhean, R. Mahendraparvata: An early Angkor-period capital defined through airborne laser scanning at Phnom Kulen. *Antiquity* **2019**, *93*, 1303–1321. [CrossRef]
36. Canuto, M.A.; Estrada-Belli, F.; Garrison, T.G.; Houston, S.D.; Acuña, M.J.; Kováč, M.; Marken, D.; Nondédéo, P.; Auld-Thomas, L.; Castanet, C.; et al. Ancient lowland Maya complexity as revealed by airborne laser scanning of northern Guatemala. *Science* **2018**, *361*, eaau0137. [CrossRef]
37. Evans, D. Airborne laser scanning as a method for exploring long-term socio-ecological dynamics in Cambodia. *J. Archaeol. Sci.* **2016**, *74*, 164–175. [CrossRef]
38. Cap, B.; Yaeger, J.; Brown, M.K. Fidelity tests of LiDAR data for the detection of ancient Maya settlement in the Upper Belize River Valley, Belize. *Res. Rep. Belizean Archaeol.* **2018**, *15*, 39–51.
39. Doneus, M.; Briese, C.; Fera, M.; Janner, M. Archaeological prospection of forested areas using full-waveform airborne laser scanning. *J. Archaeol. Sci.* **2008**, *35*, 882–893. [CrossRef]
40. Doneus, M.; Briese, C.; Kühtreiber, T. Flugzeuggetragenes Laserscanning als Werkzeug der archäologischen Kulturlandschaftsforschung. Das Fallbeispiel "Wüste" bei Mannersdorf am Leithagebirge, Niederösterreich. *Archäologisches Korresp.* **2008**, *38*, 137–156.
41. Doneus, M.; Briese, C.; Studnicka, N. Analysis of Full-Waveform ALS Data by Simultaneously Acquired TLS Data: Towards an Advanced DTM Generation in Wooded Ar. In Proceedings of the 100 Years ISPRS, Advancing Remote Sensing Science: ISPRS Technical Commission VII Symposium, Vienna, Austria, 5–7 July 2010; pp. 193–198.
42. Doneus, M.; Kühtreiber, T. Airborne laser scanning and archaeological interpretation–bringing back the people. In *Interpreting Archaeological Topography: Airborne Laser Scanning, 3D Data and Ground Observation*; Opitz, R.S., Cowley, D., Eds.; Oxbow Books: Oxford, UK, 2013; pp. 32–50. ISBN 978-1-84217-516-3.
43. Doneus, M. Openness as Visualization Technique for Interpretative Mapping of Airborne Lidar Derived Digital Terrain Models. *Remote Sens.* **2013**, *5*, 6427–6442. [CrossRef]
44. Trinks, I.; Neubauer, W.; Doneus, M. Prospecting Archaeological Landscapes. In *Progress in Cultural Heritage Preservation: 4th International Conference, EuroMed 2012, Limassol, Cyprus, 29 October–3 November 2012*; Ioannides, M., Fritsch, D., Leissner, J., Davies, R., Remondino, F., Caffo, R., Eds.; Springer: Berlin/Heidelberg, Germany, 2012; pp. 21–29. ISBN 978-3-642-34234-9_3.
45. Mandlburger, G.; Otepka, J.; Karel, W.; Wagner, W.; Pfeifer, N. Orientation and Processing of Airborne Laser Scanning data (OPALS)–concept and first results of a comprehensive ALS software. In Proceedings of the ISPRS Workshop Laserscanning '09,

Paris, France, 1–2 September 2009; Bretar, F., Pierrot-Deseilligny, M., Vosselman, G., Eds.; Société Française de Photogrammétrie et de Télédétection: Marne-la-Vallée, France, 2009.
46. Pfeifer, N.; Mandlburger, G.; Otepka, J.; Karel, W. OPALS–A framework for Airborne Laser Scanning data analysis. *Comput. Environ. Urban Syst.* **2014**, *45*, 125–136. [CrossRef]
47. Pingel, T.J.; Clarke, K.; Ford, A. Bonemapping: A LiDAR processing and visualization technique in support of archaeology under the canopy. *Cartogr. Geogr. Inf. Sci.* **2015**, *42*, 18–26. [CrossRef]
48. Kraus, K. Interpolation nach kleinsten Quadraten versus Krige-Schätzer. *Österr. Zeitschr. Vermess. Geoinf.* **1998**, *86*, 45–48.
49. Bollandsås, O.; Risbøl, O.; Ene, L.; Nesbakken, A.; Gobakken, T.; Næsset, E. Using airborne small-footprint laser scanner data for detection of cultural remains in forests: An experimental study of the effects of pulse density and DTM smoothing. *J. Archaeol. Sci.* **2012**, *39*, 2733–2743. [CrossRef]
50. Norstedt, G.; Axelsson, A.-L.; Laudon, H.; Östlund, L. Detecting Cultural Remains in Boreal Forests in Sweden Using Airborne Laser Scanning Data of Different Resolutions. *J. Field Archaeol.* **2020**, *45*, 16–28. [CrossRef]
51. Doneus, M.; Shinoto, M.; Herzog, I.; Nakamura, N.; Haijima, H.; Ōnishi, T.; Kita'ichi, S.; Song, B. UAV-based Airborne Laser Scanning in densely vegetated areas: Detecting Sue pottery kilns in Nakadake Sanroku, Japan. New Global Perspectives on Archaeological Prospection. In Proceedings of the 13th International Conference On Archaeological Prospection, Sligo, Ireland, 28 August–1 September 2019; Bonsall, J., Ed.; Archaeopress: Oxford, UK, 2019; pp. 220–223, ISBN 978-1-78969-306-5.
52. Campana, S. Drones in Archaeology. State-of-the-art and Future Perspectives. *Archaeol. Prospect.* **2017**, *24*, 275–296. [CrossRef]
53. Risbøl, O.; Gustavsen, L. LiDAR from drones employed for mapping archaeology–Potential, benefits and challenges. *Archaeol. Prospect.* **2018**, *25*, 329–338. [CrossRef]